Validation of simulation with enhanced kaon production to investigate kaon background for LDMX.

Author: Lisa Andersson Loman
Supervisor: Ruth Pöttgen

Thesis submitted for a Master of Science degree
Project conducted at full-speed during 12 months
Examination date: January 2023

LUND
UNIVERSITY

Department of Physics
Division of Particle Physics

Acknowledgements

First of all, I would like to thank my supervisor Ruth for all the support during this project, your guidance was the key to the making of this paper. And thanks to Amina Li and Natalia Toro for providing scripts to get everything started and for your insights into what UpKaons actually do. Also thanks to Einar for all the de-bugging, Hannah and Erik for help making my plots look nicer, and Lene Kristian for helping me to run the simulations on Aurora. And a special thanks to all the people present at the test beam at CERN, I learned a lot!

Abstract

Dark matter is one of our universe's largest mysteries and very little is known about what it is. One of the dominating theories, that it originates from an early universe thermal relic, indicates that it has interaction with the Standard Model. If this is the case, dark matter can be produced at accelerators and detected indirectly by searching for missing momentum signals. LDMX will join this search for dark matter with a fixed target experiment at the LCLS-II electron beam line at SLAC starting in 2025. It will initially run with a beam energy of 4 GeV, to then increase the beam energy to 8 GeV in the following upgrades to improve the signal-to-background ratio.
While searching for dark matter signals, rejecting background that might disturb the detection is crucial. In previous studies, it has been found that kaons, especially charged ones are the most difficult to filter out. The interactions that produce kaons are rare, so to investigate their behavior the production of kaons has been artificially boosted in a Geant4 simulation.

This thesis will look closer into the kaons produced in simulations where the kaon production is boosted and the beam energy is increased to 8 GeV, to make sure that adding an enhancement factor will not introduce any unphysical or uncharacteristic behavior.

Contents

Abbreviations

LDMX Light Dark Matter eXperiment
DM Dark Matter
SLAC Stanford Linear Accelerator Center
pn photonuclear
CP charge conjugation parity **ECal** Electromagnetic Calorimeter
SM Standard Model
LESA Linac to End Station A
EoT Electrons on Target
HCal Hadronic Calorimeter
p_T Transverse momentum
X_0 Radiation length
TS Trigger Scintillator
LYSO Lutetium-yttrium oxyorthosilicate
CMS Compact Muon Solenoid
BDT Boosted Decision Tree
MIP Minimum Ionizing Particle
SiPMs Silicon Photomultipliers
kf Kaon Enhancement factor

Chapter 1

Introduction

The Light Dark Matter eXperiment (LDMX) is an upcoming experiment searching for dark matter (DM) in a "light" mass range that remains fairly unexplored though it is well motivated by DM models. LDMX is an electron beam fixed-target experiment designed to measure missing momentum in the search for DM. It is planned to collect data at a dedicated beam-line at LCLS-II at Stanford Linear Accelerator Center (SLAC) National Accelerator Laboratory with a start in 2025. Initially, the experiment will run with a beam energy of 4 GeV but is planned to also run with 8 GeV at a later stage. For the study in this paper, the 8 GeV upgrade is considered. Increasing the beam energy to 8 GeV would extend the explorable mass range and allow the parameter space below $\sim$1 GeV to be explored, hence improving the possibilities of finding DM [1]. However, increasing the beam energy also might raise new challenges in vetoing the background.

Previous LDMX studies have shown, using simulated data with a beam energy of 4 GeV, that the most challenging events to veto are photonuclear (pn) events where a photon undergoes a rare interaction that transfers most of its energy to charged kaons (K^- and K^+) that decays in flight [1]. In such a decay chain most of the energy ends up escaping the detector with a neutrino and this type of interaction leaves only a short track in the electromagnetic calorimeter (ECal). This interaction has a possibility to be misinterpreted as a missing momentum signal left by a DM particle in the detector. When performing LDMX runs at higher luminosity and higher beam energy, the rates of key background topologies fall steeply, making the signal-to-background ratios higher. This seems promising but are there any downsides to going to higher energies?

The focus of this study is on the kaon background. Pn reactions producing kaons are rare processes but they could be difficult to veto. Therefore, to get enough statistics, a bias has been added to the regular simulations. With a higher number of kaons, it is easier to study their behavior and the tracks they might leave in the detector as an important tool to fine-tune the vetoing strategies for the 8 GeV upgrade of LDMX. The study in this thesis deals with an essential step on the way, validating that the changes made to increase the number of kaons have not introduced any unphysical behavior that may interfere with the analysis. Depending on the results, some optimization processes might be needed to successfully veto the kaon background at 8 GeV and meet the goal of the zero background for

the experiment. Some studies have already been made with this modified Geant4 version simulating a beam energy of 4 GeV, however, this study will focus on a beam energy of 8 GeV.

Chapter two will introduce the LDMX detector and the experiment, and Chapter three will introduce the physics that is the foundation for the motivation of LDMX and the study conducted in this thesis. In Chapter four the simulations performed are introduced and presented, as well as the changes implemented for the enhanced kaon simulations. Chapter five presents the results and the analysis and Chapter six sums it all together and gives an overview of what is needed next based on the outcomes of this study.

Chapter 2

LDMX

2.1 DM signal and background

The missing momentum search for DM in LDMX will be sensitive to any process in which a beam electron transfers most of its energy to "invisible" particles and at the same time receives a significant transverse push in the production of the invisible particles. The most relevant processes, which result in a DM signal with such an experimental signature, are presented in Fig 2.1.

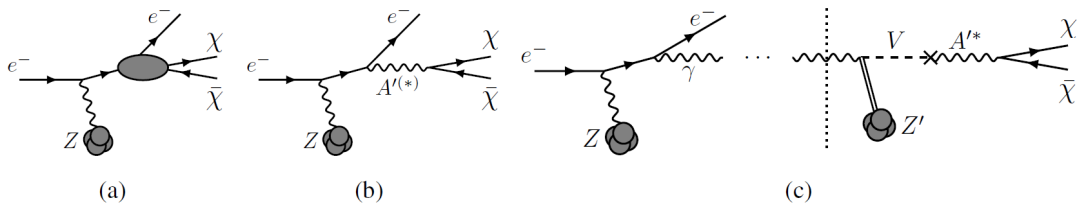

Figure 2.1: Schematic image of possible DM signals [2]. 2.1(a) represents dark bremsstrahlung, where an electron scatters off a nucleus and produces a pair of DM particles directly through effective interaction. In Figure 2.1(b) the DM particle is produced in a similar process but instead through the production and decay of a mediator particle A' (dark photon). There is also the case of photo-production of vector mesons from a hard bremsstrahlung photon that scatters off a nucleus (Figure 2.1(c)), which then later decays invisibly to DM particles via mixing with a mediator A'.

When electrons from the beam interact in the target with known processes creating Standard Model (SM) particles it is classified as background. Most of the background is electrons that do not undergo any hard interactions in the target, but typically deposit the full beam energy in electromagnetic showers in the ECal. The leading source for low-energy electrons that counts as background comes from events in which the incoming beam electron undergoes hard bremsstrahlung when colliding with the target, producing a multi-GeV photon. These photons usually initiate electromagnetic showers that deposit a large amount of energy in the ECal. But there are also rare processes, if this photon undergoes secondary interactions

it can produce more complicated final states which possibly can mimic a missing momentum signal [1]. This could be pn reactions or photon to muon ($\gamma^* \rightarrow \mu^+\mu^-$) conversions in the target or in the ECal that result in low energy deposits in the ECal. Most of these interactions and the secondary particles that can be created leave type-specific signatures in the ECal, hadronic calorimeter (HCal), and/or recoil tracker, which allows them to be identified and vetoed. However, these secondary interactions can also produce more complicated final states which possibly can mimic a missing momentum signal. As an example, charged kaons are deemed as difficult as one of their decay products is a neutrino whose interaction can fake the missing momentum signal.

The DM signal is characterized by a single low-energy recoil electron while most of the beam energy is carried away by dark matter. For 4 GeV the cut of the recoil electron lies at < 1.5 GeV, corresponding to a missing energy of at least 2.5 GeV. For 8 GeV the energy cut on the recoil electron is ~ 3 GeV.

2.2 The experiment

LDMX is a proposed fixed-target experiment designed to search for DM in the sub-GeV mass range, motivated by the possibility that DM originates from the early universe. Thermal relic DM can explain current observations if the mass were to be roughly between 1 MeV and 100 TeV. Within this theory, which is presented in more detail in 3.1, interactions necessary for DM to thermalize with SM particles indicate that DM production at particle accelerators is possible. Hence, for LDMX, DM is in itself produced in the collision between the electrons in the electron beam and the thin tungsten target, and could then be detected by measuring missing momentum. LDMX presents a high sensitivity to sub-GeV light DM [2] and the sub-GeV mass range of the parameter space is well motivated. This makes it an important piece in the test of the thermal relic explanation for dark matter.

LDMX will make use of the electron beamline LCLS-II at SLAC, with a beam energy of 4 GeV in the initial stage and an integrated luminosity matching to test the thermal targets for different models across a range of DM masses. The beam will be ready to be delivered at the beginning of 2025 by The Linac to End Station A (LESA) at SLAC [2]. With a successful beam test session at CERN in 2022 and a successful physics review in the summer of the same year, the realization of the experiment is near. A veto study for the initial 4 GeV beam energy has been conducted [1], presenting that the experimental set-up and veto strategy for LDMX will reach a high sensitivity while successfully rejecting background events. A similar study for the upgrade with a beam energy of 8 GeV will be presented in 2023.

In the first phase of running, LDMX is expecting to collect a sample of 4×10^{14} electrons on target (EoT) over the span of a year, and in the second phase, the beam energy will increase from 4 GeV to 8 GeV, delivering 10^{16} EoT over the following years.

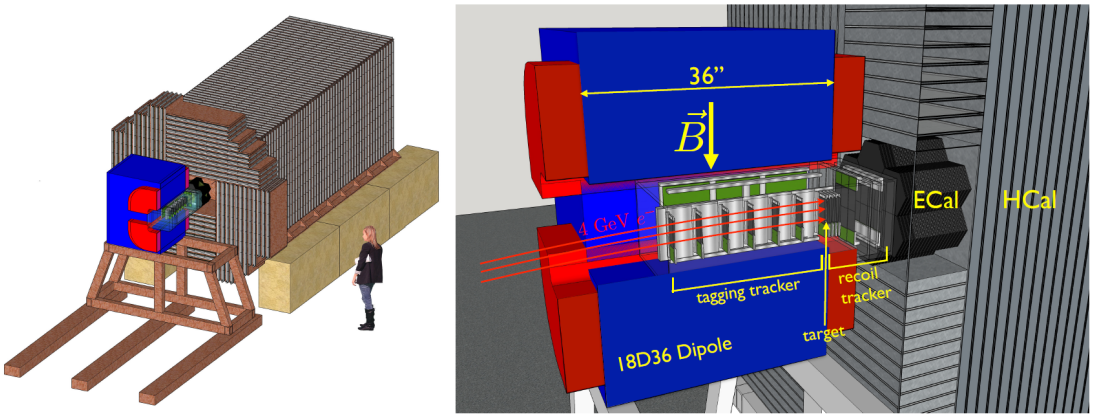

Figure 2.2: The design of the LDMX main detector with human for scale [2]. To the right, some layers of the detector have been removed to reveal the layout of the subdetectors.

A schematic view of the detector can be seen in Figure 2.2. A three-dimensional coordinate system is defined as z being along the beamline, y being vertically perpendicular to z, and x being horizontally perpendicular to z. The detector simplistically consists of trackers, an Electromagnetic calorimeter (ECal), and a Hadronic calorimeter (HCal) to capture the complete picture of particle showers. All the subdetectors will contribute to the rejection of background and detection of possible DM through missing momenta measurements. It is designed to be able to collect a large dataset from a single-electron scatter on a thin target, and then completely reconstruct the particle interactions with the downstream subdetectors.

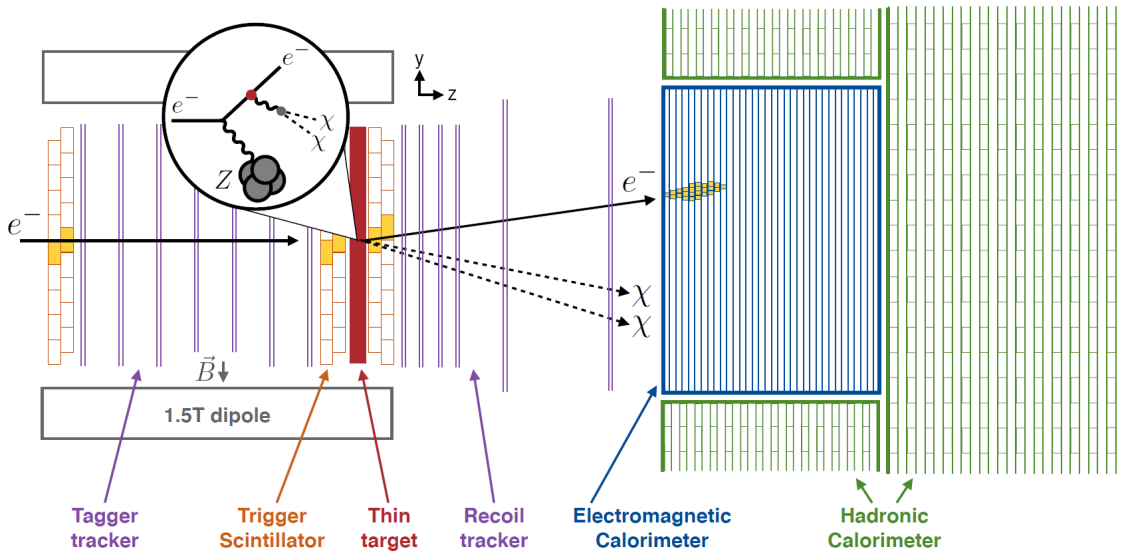

Figure 2.3: Sketch showing the path of the beam electron as it interacts with the target and produces a DM signal. The general design of the subdetectors is also shown. The image is not to scale. [2]

A signal event is defined as a single low transverse momentum (p_T) recoil electron, while there is a complete absence of other particle activity in the event, as illustrated in Fig 2.3. If one were to discover such events, the DM will be characterized through the missing momentum spectrum that will be measured, introducing a relevant mass range to be used in future DM searches. For this to be possible, a goal has been set to veto all backgrounds, while retaining as high signal efficiency as possible, which is crucial to be able to detect a DM signal. In Fig 2.4 the sensitivity is graphically represented with thermal targets in the dark photon model with different types of dark matter. A high signal efficiency together with a zero background allows LDMX to probe several key thermal targets in the 1-100 MeV mass range during the first 4 GeV run of data taking, and up to several 100 MeV in Phase 2 of data taking.

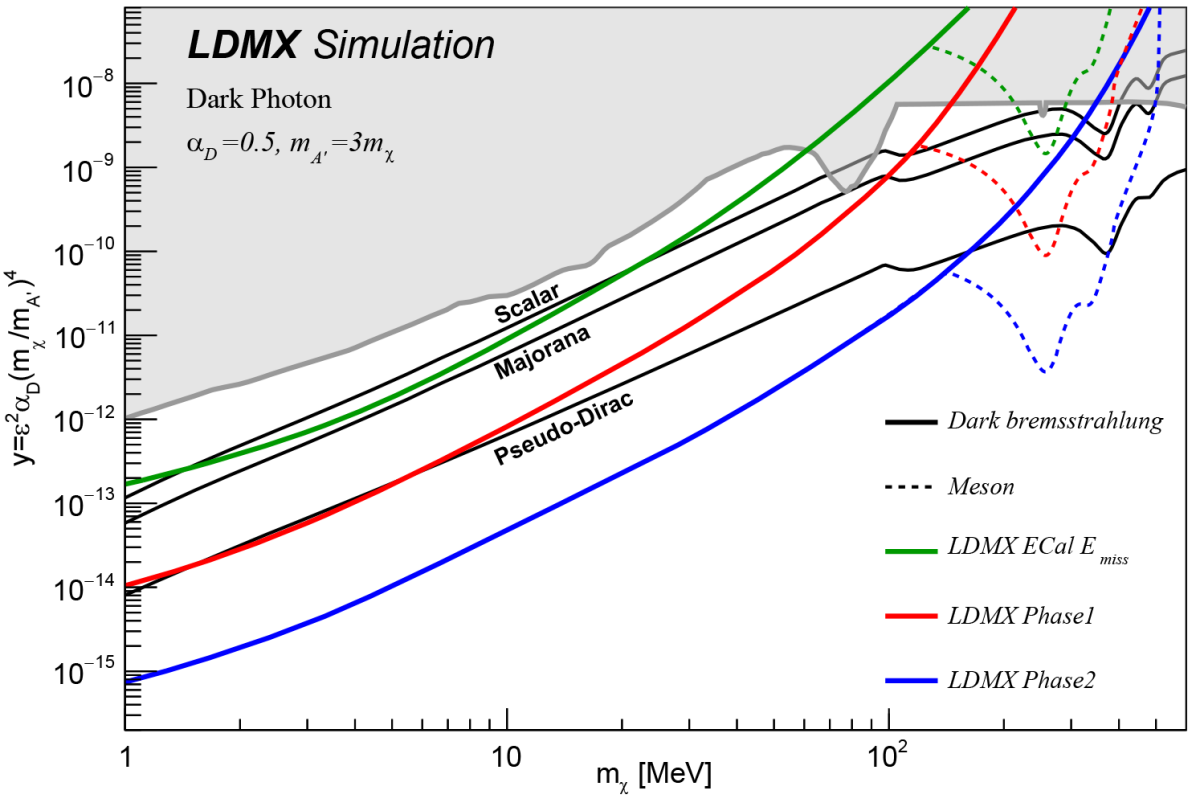

Figure 2.4: Sensitivity plot in the y vs. m_χ plane. y is the interaction strength and m_χ is the mass of dark matter. The missing momentum reach is represented by the red line for Phase 1 with a 4 GeV beam energy and the blue line represents Phase 2 with an 8 GeV beam energy. The benchmark thermal relic targets are represented by black lines and the grey region is a constraint from previous DM experiments. For the constraints, it is assumed that the mediator mass ($m_{A'}$) is three times the DM mass (m_χ), and its coupling constant is $\alpha_D = 0.5$ [2].

The benchmark for LDMX is a direct annihilation model where the population of DM particle χ is reduced in the early universe through annihilation to standard model fermions f via a sector mediator A', a mediator to the dark sector.

$$\chi\chi \rightarrow A' \rightarrow ff$$

The nature of the DM particle varies depending on the model considered (i.e. scalar, fermion, or not just one particle) but this will generally not impact the phenomenology of the missing momentum search in LDMX (Fig. 2.4). In LDMX, there will be a focus on DM produced by dark bremsstrahlung from the decay of the new U(1) gauge boson A', the dark photon, which is representative of other dark matter models.

Probing the existence of thermal relic DM in the sub-GeV mass region is well-motivated and is an important part of a fully realized search program for DM [2]. By conducting missing-momentum searches while colliding electrons with an energy of 4-8 GeV, LDMX's intention is to find some pieces of the puzzle, rule out some theories or models, and/or tighten the mass limits for future experiments.

2.3 The Detector

2.3.1 Target

The beam of electrons will be focused on a thin tungsten target, 350 μm thick, corresponding to 0.1 radiation length (X_0) [1]. This thickness has not been optimized but it is chosen to provide a balance between signal rate and good p_T resolution from multiple scattering. The target is glued to two scintillator plates for a fast estimate of the number of incoming electrons at the trigger level. The electron beam will hit the target and the electrons will interact to produce DM and cause particle showers in the detector. The type of interactions that takes place is, for instance, electronuclear and photonuclear processes that transform visible energy to secondary particles such as neutrons and kaons that are more difficult to detect. These various particles will be vetoed in different subdetectors in the detector.

2.3.2 Tracking/Trigger system

The main purpose of the tracking system is to measure electron momenta with high precision before and after passing through the target. The tagging tracker system, which can be seen in Fig 2.3, consists of stereo silicon strip modules located within a 1.5 T dipole magnet upstream of the target. One of the sensors in these stereo modules is oriented vertically, for good momentum resolution, and the other is oriented at a stereo angle of $\pm 100\, mrad$ to give better position resolution. 7 of these double-sided modules are placed in front of the target, with a distance of 10 cm between each layer, to filter out electrons that have an energy that is below the beam energy. The large distance between the layers ensures precise measurement of the momentum, and the multiple numbers of layers provide a mean for pattern recognition.

After the target, there is a similarly constructed recoil tracker, located in the fringe field of the magnet. Its purpose is to identify and precisely measure recoil electrons with low momentum (50 MeV to a few GeV). Here there are four layers of the same modules that are used in the tagging tracker before the target. The spacing between these is 1.5 cm and will

provide a good pattern recognition for particles with very low momentum. In addition, two single-sided modules, with vertically oriented strips, are located 9 and 18 cm from the target. This is to provide an optimized momentum measurement over the entire valid momentum range.

The Trigger Scintillator (TS) identifies fiducial beam electrons in real-time. The TS will consist of plastic or Lutetium-yttrium oxyorthosilicate (LYSO) bars and is located before the tagger tracker and on either side of the target.

2.3.3 ECal

The electromagnetic calorimeter for LDMX needs a fast readout, good energy resolution, and especially good spatial resolution to precisely reconstruct charged particle showers. This is crucial to be able to distinguish between signal and rare background events that have a small observable energy deposit in or near the bremsstrahlung photon's shower region in the ECal. To be able to achieve this, a high-granularity silicon-tungsten sampling calorimeter will be used. It is made up of 17 double layers, each consisting of two silicon-tungsten layers and a cooling plane in between. The thickness of the tungsten layers varies from 1mm to 7mm which adds up to a total of 14 cm, corresponding to 40 X_0. The 34 layers that make up the ECal are arranged in a flower pattern using hexagonal shapes. Even though the ECal design is based on the high-granularity calorimeter developed for the Compact Muon Solenoid (CMS) experiment at CERN, there are differences to the modules, optimized to better suit LDMX's search goals [3].

A DM signal is characterized as a low-energy recoil electron while there is an absence of other particles. Hence, in the case of a DM particle, there is a low-energy deposit expected in the ECal. If there was a background event, most of the beam energy would be expected to be converted to electromagnetic showers in the ECal. This expectation results in a primary trigger strategy with an upper threshold for the reconstructed energy in the ECal. The TS system provides information about the total number of incoming beam electrons in a time sample which determines the missing energy threshold for the trigger. For 4 GeV, with a single electron event, this threshold is 1.5 GeV requiring the missing energy signal to be at least 2.5 GeV [1]. There is also a corresponding offline selection where it is required that the reconstructed energy of the full ECal also meets the threshold of 1.5 GeV.

2.3.4 HCal

The HCal is a large construction consisting of scintillators and steel absorbers between the scintillating layers. The scintillators have a similar design to what is used for the Mu2e Cosmic Ray Veto System [1], though it has been optimized using detailed Geant4 simulations to specifically meet the requirements for LDMX [1]. The HCal consists of approximately 90 layers of 25 mm steel absorber plates and 20 mm scintillators in between. This will add up to a length corresponding to $\sim$15 X_0 [1]. The scintillators are polystyrene-doped,

20 mm × 50 mm× 2m bars, read out at both ends using Silicon Photomultipliers (SiPMs) [2].

To be able to detect particles at large angles, there is also an HCal on either side of the ECal. The side HCal is similar to the back HCal in design.

The main purpose of the HCal is to identify neutral hadrons, mostly neutrons but also neutral kaons, produced in the target or the ECal. It needs to do so with very high efficiency in an energy range from approximately 100 MeV to a few GeV. It must also be sensitive to MIPs (such as muons) and be able to measure the component of electromagnetic showers that are escaping from the ECal.

Worth noting is that there is still ongoing work to optimize all the subsystems.

2.4 Veto/background rejection

In most experiments, there are particles created that are of no interest to the experiment at hand and may interfere in the search for the signal. It is of utter importance that an experiment is designed with this in mind and has a well-developed strategy for distinguishing between signal and background. This DM experiment is no different. LDMX has as a goal to be able to veto all backgrounds, an important step to be able to distinguish DM from SM particles. In this case, an electron beam is aimed toward a tungsten target initializing multiple interactions. The success of finding a dark matter signal lies in being able to discard SM interaction, no matter how rare they are or how tiny tracks they leave in the detector. The main point is, it is difficult to find signs of dark matter, therefore finding strategies for vetoing background when collecting data is crucial.

As LDMX aims to be a zero-background experiment and has multiple steps in the veto strategy. For instance, the track veto uses the definition of a signal event, hence a single track in the recoil tracker induced by an electron. Also, any secondary particle from pn reactions that reaches the HCal is a sign that it is a background event, as no energetic second particles are expected from the electron shower in the signal event.

Apart from the primary trigger with the energy deposition threshold in the ECal, track selection is also important. We require a single track in the recoil tracker with a momentum smaller than 1.2 GeV. This helps to suppress backgrounds with a hard bremsstrahlung photon that interacts with the target; interactions that could be photon-to-muon conversion, photonuclear, or electronuclear reactions, which all may result in additional tracks. Some of these tracks survive the track selection and the missing energy threshold and have to be vetoed in some other way. The dominant surviving background is events where the beam electron undergoes hard brehmsstrahlung in the target, the photon emitted in this interaction then subsequently undergoes muon conversion or a pn reaction in the target or in the ECal.

To reject even more events, an ECal-boosted decision tree (BDT) is introduced. This is a machine learning tool that we train on simulations where we tell it which of the events are background and which of the events are signal. This then returns a score which is a measure of signal or background. The BDT variables are chosen based on information about the energy deposition in the ECal. The BDT can veto both events with photonuclear interactions in the ECal and backgrounds with target pn interactions or muon conversions that have survived the energy thresholds and the track selection. For instance, pn events typically deposit their energy deeper in the ECal and have a broader transverse shower profile than signal events. There are also BDT variables related to containment regions, areas in the ECal that have a higher possibility of containing most of the shower energy from the recoil electron, and other activity related to the background. The BDT discrimination is designed to be uncorrelated with the transverse momentum of the recoil electron.

There is also a veto possibility in the HCal both for pn reactions and muon conversions. Pn reactions can produce hadronic showers and the muons from the muon conversions can penetrate the HCal which will usually result in a large number of hits in the HCal. The HCal veto is also of most importance when it comes to vetoing pn events where most of the energy is carried away by a single, energetic, forward neutral hadron, such as a neutron or a K_L^0. The HCal is therefore optimized to veto such events.

The remaining background is mainly charged kaons, produced in pn reaction and decaying in flight in the ECal to a muon and a neutrino. Most of the energy goes in the neutrino and the only visible track in the detector from such an event might be a short track in the Ecal that the kaon makes before decaying. The high granularity of the ECal makes it possible to identify MIP tracks. There is a dedicated algorithm that identifies tracks and isolated hits from charged particles from photon interactions in the ECal. This is a way to reject the remaining pn background of charged kaons that survives all other veto strategies.

In the 4 GeV study, it has been shown that collectively these veto handles result in less than 1 background event in a 4×10^{14} EoT sample. This is based on a Geant4 simulation of events with >2.8 GeV photons using a 4 GeV electron beam. If this performance is matched in the 8 GeV case it would allow LDMX to probe a wider range of thermal targets, which is presented in Figure 2.4.

2.5 From 4 GeV to 8 GeV

Searching for light DM with LDMX produced in fixed-target 4 GeV electron beam collisions has been the main focus in most of the LDMX studies, however, there is a clear benefit to moving to higher energies, to improve sensitivity, see Figure 2.4. This is because moving to higher energies, sensitivity is extended while the rates for some of the more challenging final states of pn interactions scale with $1/E_\gamma^3$ [2]. That is, higher beam energy makes it easier to distinguish between SM reactions that fake the missing momentum signature and signal events.

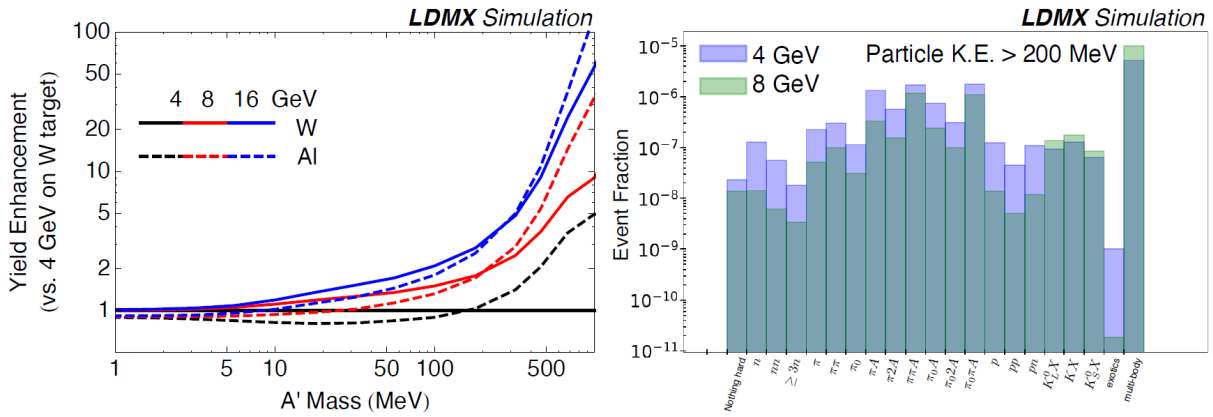

Figure 2.5: Shown in the left plot is the yield enhancement as a function of dark photon (A') mass. The black lines show the 4 GeV case, red is for a beam energy of 8 GeV and blue is for 16 GeV. The solid lines show the possibilities with a tungsten (W) target and the dashed lines show the scenario if an Aluminium target would be used instead. To the right is a plot of the fraction of pn events for the 4 GeV beam energy and the 8 GeV beam energy. Note that almost all low-multiplicity final states occur less often when the energy is increased, except for the kaons [2].

In Figure 2.5 it can be seen that the fraction of pn background events decreases in almost all cases when increasing the beam energy from 4 GeV to 8 GeV. However, the situation is reversed for the kaons, motivating a study of the kaon background with a beam energy of 8 GeV.

Chapter 3

Physics/motivation

As complete as the standard model might be, SM particles only make up for about 5% of the matter in the universe. Out of the remaining mass, 27% is DM and 68% is dark energy [4]. The first signs that there was something beyond the SM were realized in 1933, by Fritz Zwicky when measuring the velocities of galaxies in the Coma cluster. The mass he measured was about 400% larger than the visible mass (stars in the cluster). The conclusion was drawn that galaxies contained mass that did not radiate, hence it was called dark matter.

Another, more recent evidence of dark matter is the rotational curves of velocity vs radial distance for stars and gas in our galaxy [5]. If we consider a star of mass m at distance r from the center of a galaxy, with the mass of the galaxy being M. The star is moving with a tangential velocity v. According to Newton's law of universal gravitation, $F = G\frac{mM}{r}$, the velocity v of a star that is a substantial distance away from the center of the galaxy, should decrease with $1/\sqrt{r}$. However, this velocity is instead increasing, suggesting that dark matter exists as an extended halo outside the galactic nucleus.

Even though the first indications of dark matter were observed nearly 100 years ago, a solution to what it is composed of has not been discovered. Is it one particle? Neutrinos? Something completely new? A combination of all of the above? In this thesis, it is considered that dark matter is a thermal relic from the early universe with a mass range from sub-MeV to 100 TeV.

3.1 "Light" dark matter

As mentioned previously, dark matter could be a lot of things, though to allow it to be probed in accelerator experiments there needs to be some connection to the standard model. One prominent theory, that LDMX rests upon, is that DM originates as a thermal relic from the early hot universe [3]. This explanation requires that there is a small non-gravitational connection between DM and SM matter, extending beyond the standard model.

The interest in searching for dark matter in the "light" mass region ($\sim$ 1 MeV to 1 GeV) has emerged over the last years from ideas that there is a dark sector that is neutral under

SM forces. This means that there are no strong, weak, or EM interactions taking place, but still some new interactions with SM matter. For the benchmark model in LDMX, a new U(1) gauge boson, the dark photon, A', is considered as a new mediator particle, described in Section 2.1.

This explanation indicates that there is a production mechanism for DM at accelerators. LDMX with its missing momentum measurement, will join the search for DM in the mass range from 1-100 MeV in the initial phase of data taking, probing multiple key thermal targets, see Figure 2.4.

3.2 Photonuclear reactions

Photonuclear (pn) reactions are reactions where photons react with nucleons. Although it is more common that photons interact with atomic electrons, or are affected by the nuclear field surrounding the nucleus without actually penetrating it, photons with high energy can penetrate the nucleus and result in the emission of nucleons, α particles, or kaons which is the main focus of this thesis.

Although these are rare processes, there are two main reasons for focusing on the background of pn reactions in LDMX. **First:** Hard bremsstrahlung is the leading source of low-energy electrons in the experiment, hence the photon emission is large. The photon-initiated background, therefore, is the largest single background for the experiment, and its rejection is crucial to LDMX's performance. **Second:** Photon-initiated background rejection is highly representative of the capabilities to reject background processes produced directly by the incident electron. So, if background from the pn reactions can be vetoed, background from other processes will most likely be able to be vetoed as well.

3.3 Kaons

The kaons are strange mesons, namely particles consisting of an even number of quarks where at least one of them is a strange one. There are four different types and we can expect all of them as products of pn reactions in LDMX. The quark content of the kaons for K^- is $(s\overline{u})$, for K^+ it is $(u\overline{s})$ and for the neutral kaons $(d\overline{s})$.

The production of these strange particles can be expected to increase with beam energy since higher energy is available for the reactions. Hence, a higher fraction of kaons can be expected at 8 GeV than in the 4 GeV initial phase.

3.3.1 Neutral kaons

K_L^0 (K-long) is a neutral hadron with a lifetime of 5.2×10^{-8} s [6]. K_S^0 (K-short) has, as the name indicates, a shorter lifetime, namely 8.9×10^{-11} s. The difference between them has its explanation in Neutral Kaon Mixing [7]. A two-pion configuration has a parity of +1 and

a three-pion configuration has a parity of -1. Hence neutral kaons can decay to two or three pions. The decay to two pions is much faster because the energy release is greater, implying that the neutral kaon that decays to two pions is called K_S^0 and the one that decays to three pions is called K_L^0. There are some circumstances that allows K_S^0 to rarely decay to 3 pions (still conserving $CP = +1$) but K_L^0 can never go to two pions [7].

The most common decay channels for K_S^0 is;

$$K_S^0 \to \pi^0 + \pi^0 \text{ and } K_S^0 \to \pi^+ + \pi^-$$

and for K_L^0 it is;

$$K_L^0 \to \pi^+ + \pi^- + \pi^0 \text{ or } K_L^0 \to \pi^0 + \pi^0 + \pi^0$$

3.3.2 Charged kaons

The charged kaons have the same lifetime, namely 1.2×10^{-17} s. The charged kaons have both leptonic and hadronic decay modes with are presented below together with their branching ratio (BR) [8];

$$\text{Leptonic: } K^+ \to \mu^+ + \nu_\mu \text{ or } K^- \to \mu^- + \overline{\nu}_\mu \text{ (BR: } 63.56 \pm 0.11)$$

$$\text{Semi-leptonic: } K^+ \to \pi^0 + e^+ + \nu_e \text{ and } K^+ \to \pi^0 + \mu^+ + \nu_\mu \text{ (BR: } 5.07 \pm 0.04 \text{ and } 3.352 \pm 0.033)$$

$$K^- \to \pi^0 + e^- + \overline{\nu}_e \text{ and } K^- \to \pi^0 + \mu^- + \overline{\nu}_\mu \text{ (BR: } 5.07 \pm 0.04 \text{ and } 3.352 \pm 0.033)$$

$$\text{Hadronic: } K^+ \to \pi^+\pi^+\pi^- \text{ or } K^- \to \pi^+\pi^-\pi^- \text{ (BR: } 5.583 \pm 0.024)$$

$$K^+ \to \pi^+\pi^0 \text{ or } K^- \to \pi^-\pi^0 \text{ (BR: } 20.67 \pm 0.08)$$

The decays that are especially troublesome are the leptonic decays, where the decay products of a charged kaon include a neutrino. The energy that goes into the neutrino can be mistaken as a signal event as a neutrino leaves no trace in the LDMX detector.

Chapter 4

Simulations

LDMX has its own software framework called ldmx-sw [9], which is a collection of software tools used for the simulations which are mostly written in C++ code. ldmx-sw uses Geant4 [10] as a simulation package to simulate the response of the detector when particles pass through it. Simplistically, Geant4 needs two things to run the simulations, it needs to be told what to simulate and what to pass it through. In our case, it is an 8 GeV electron beam incident on a tungsten target and then passing the reaction products through the LDMX detector. All this information is given through a configuration file where all the information is provided.

As mentioned previously, pn reactions producing kaons are rare events but the kaons are difficult to veto, especially the charged ones that decay leptonically. To be able to study the behavior of the kaon background, simulations have been performed using a modified Geant4 [10] toolkit developed for LDMX (called UpKaons) which enhances the kaon production. In this modification, there is more than one thing happening. The production rate of kaons from pn reactions is increased by scaling up the cross-sections, both for charged and neutral kaons. This enhancement factor can be regulated from 0 to 30 in the simulation. The default is set to an enhancement factor of 25 to give a substantial increase in the number of kaons produced while still leaving some distance to the upper bound. Also, a reduction to the charged kaon decay rate has been implemented with a factor of 50 and the leptonic decay branching fraction (including the semi-leptonic decays) has been increased from 0.72 to 1. These changes will increase the number of early leptonic in-flight decays by a factor of $50/.72 \sim 70$, resulting in the kaons in the biased simulations traveling a shorter distance than in an unbiased sample. This is done to be able to study short tracks in the detector, long tracks are easier to identify and veto.

The kaon production boost only affects kaons produced directly in the pn interaction, so-called primary production. In secondary production, the pn interaction produces light hadrons that then scatter in the nucleus to produce kaons. This leads to the kaons having very low energy contribution. Therefore, as a result of the enhancement factor only affecting primary production, the low energy secondary produced kaons are fewer and fewer in comparison to the primary produced kaons. Hence already from a small enhancement factor, it is enough for us to not be concerned about them. I.e the primary produced kaons will

dominate over the secondary ones. Setting the enhancement factor to 0 results in turning off the primary production of kaons completely. For this reason, a simulation using UpKaons with enhancement factor 1 is referred to as an unbiased simulation.
As an example, the difference in primary and secondary produced kaons could be that in the first case, a photon collides with a proton in the nucleus and produces kaons in some configuration. In secondary production, the photon collides with a proton in the nucleus and produces for instance a π^+ along with other particles. The π^+ particle then collides with a neutron to produce a kaon. I.e. the kaon is produced in the second step in the cascade history.

The simulation of the data has been performed on the Aurora cluster which is provided by Lunarc [11] using ldmx-sw and the Geant4 toolkit UpKaons. The detector geometry is defined in GDML files passed on to Geant4 together with other parameters needed, such as what particles to generate and at what energy (generator), additional biasing factors, etc. This is all put together in a configuration file that is run to start the simulation. It is important to give each simulation an individual run number since identical run numbers will generate the same set of data. An example of a configuration file used for the simulation is given in Appendix A.

Apart from using UpKaons and providing generator, detector version, and biasing factor in the configuration file, some additional kaon filtering has been added to produce biased interactions in the ECal. To pass the filtering and be counted as a kaon event, there must be a kaon among the interaction products. This is on top of the regular pn filtering where only events where hard bremsstrahlung occurs, and a pn reaction happens in the ECal, are considered. As well as all photonuclear tracks are tagged to persist them to the event. The file where the filtering is defined can be seen in Appendix B.

Approximately 100×10^6 events were simulated for each enhancement factor, this is defined as events started in Table 4.1. Samples were generated for enhancement factors 0-5 in steps of 1 and 5-30 in steps of 5.

Enhancement factor	Events started	Total no. of kaon events	K_L^0	K_S^0	K^+	K^-	Total no. of kaons
1	96×10^6	20124	7321	7251	9009	3581	27162
2	95×10^6	26671	10351	10316	12023	6158	38848
3	98×10^6	34549	13762	13865	15657	9012	52296
4	98×10^6	41487	16676	17116	18789	11743	64324
5	98×10^6	48017	19815	20032	21596	14176	75592
10	94×10^6	77735	33435	33416	35283	26012	128146
15	94×10^6	109341	47314	48084	49646	37873	182917
20	99×10^6	147764	64842	65077	67130	52721	249770
25	99×10^6	177791	78354	78665	80698	64368	302085
30	93×10^6	198463	87899	87998	90211	72702	338810

Table 4.1: Events started, total number of kaons and kaon events, as well as number of K_L^0, K_S^0 and $K^\pm$ respectively for enhancement factors 1-5 in steps of 1 and 5-30 in steps of 5.

The output of the simulation is given in ROOT [12] format, and by using ROOT's python interface PyROOT, the data presented in this thesis has been plotted and analyzed with Python [13] and matplotlib [14].

Chapter 5

Analysis

There is more than one parameter is being affected in the UpKaons version of the simulations and an important step in the analysis is to validate that the physics is intact. The coordinate system used is the one introduced in Section 2.2, i.e the z-direction is along the beam direction, the y-direction is the vertical direction and x is the horizontal direction. The angle θ is the angle away from the beam direction.

The variables studied in this thesis are energy, momentum, angle away from the beam direction, production location in the beam direction, endpoint in the beam direction, and the difference between the production vertex and the endpoint, i.e the length of the kaon trace. If the energy distribution is different, the BDT might be trained on an energy that is not representative of an unbiased sample. If the production location is different, then the kaons are not produced where they are expected to. The length of the tracks is of interest for the veto process, the same goes for the angle. Producing 2d plots of the variables is also a valuable safety check, for instance, we expect the particles with the largest angle to have the lowest energy and the most energetic particles to move in the forward direction. The number of kaons produced in each simulation is also analyzed to see if the input enhancement factor matches what is seen in the simulations. Also, the fraction of different kaon types are studied to make sure that this does not change since there are different veto handles for neutral and charged kaons.

5.1 Number of kaons

The events started for each enhancement factor are presented in Table 4.1 together with the number of kaons produced and the total number of events containing kaons. In analyzing the simulations, some events contained more than one kaon. The maximum number of kaons of each type is presented in Table 5.1. The numbers are not affected by the increase in the enhancement factor.

Enhancement factor	Max no of K_L^0 per event	Max no of K_S^0 per event	Max no of K^+ per event	Max no of K^- per event	Events without kaons
1	3	3	2	2	7
2	3	3	2	1	1
3	3	3	2	2	6
4	3	3	3	1	14
5	3	3	2	2	10
10	3	4	2	2	4
15	4	3	3	2	9
20	3	4	2	2	7
25	4	4	3	2	2
30	3	3	3	2	2

Table 5.1: Max no of kaons of each type in the kaon events..

It was also noticed that some events that pass the filtering have no kaons in them at all, the reason for this is currently under investigation within the LDMX collaboration. This behavior also seems to be uncorrelated to the increase in the enhancement factor.

5.2 Primary vs secondary produced kaons

There is no easy way to determine if the kaons come from primary or secondary production. Although, by producing samples for kaon enhancement factor (kf) 1-5, the effect of the boosting of only primary productions can be studied. There should be some indications that the significance of the secondary produced kaons decreases with increasing enhancement factor. There is also a simulation with an enhancement factor of 0 for comparison in these plots. Using enhancement factor 0 in the simulations represents events where the primary production is turned off completely and therefore shows a significant difference in distribution. This can be seen in Figure 5.1.

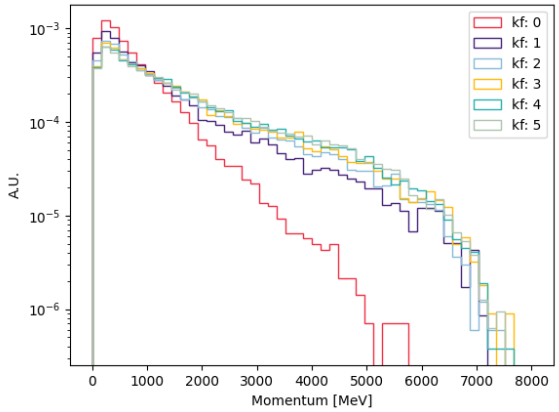

(a) Momentum K_L^0

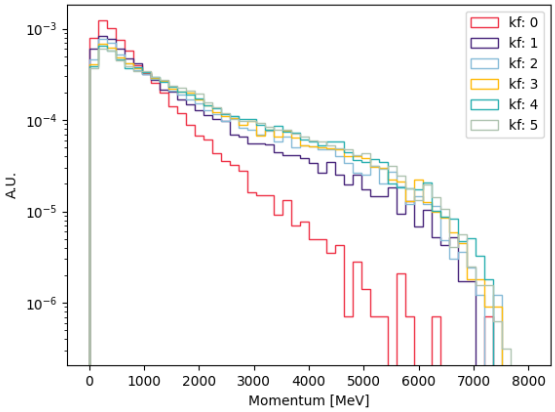

(b) Momentum K_S^0

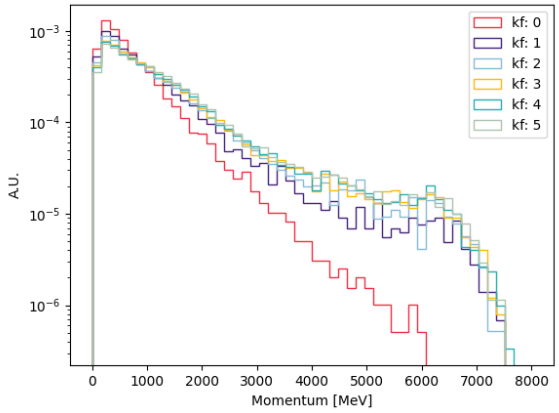

(c) Momentum K^+

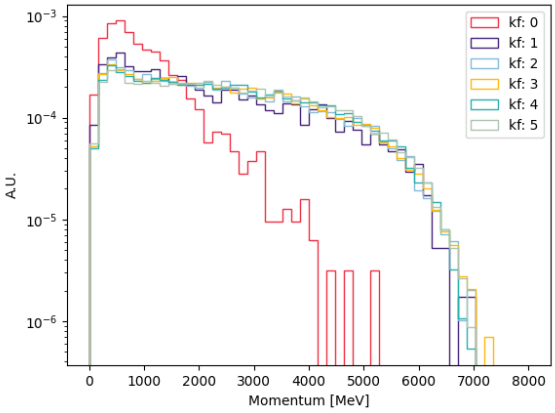

(d) Momentum K^-

Figure 5.1: Momentum of kaons produced in samples ranging from kaon enhancement factor 0 to 5 for K_L^0, K_S^0, K^+ and K^-. The shape of the distribution is changing from enhancement factor 0, where the primary production is turned off, to larger enhancement factors. The data is normalized such that the area under the histogram sums up to 1.

Figure 5.1 presents histograms of the magnitude of the momentum in MeV of the four different kaon types (K_L^0, K_S^0, K^+ and K^-) for enhancement factor 0 to 5. It is normalized in such a way that the area under the histogram sums up to 1. This makes the distributions comparable since there is a different number of events started for each enhancement factor. For all types of kaons, the momentum is lower for enhancement factor 0, which is in agreement with the fact that secondary reactions produce kaons with lower momentum.

In the simulations, the momentum is set at the production of the particle and given as a vector. Presented here is the magnitude of this vector, i.e $||p|| = \sqrt{p_x^2 + p_z^2 + p_y^2}$. With p_x being the momentum in the x-direction, p_y the momentum in the y-direction, and p_z the momentum in the z-direction.

5.2.1 Fraction of kaons

The comparison of the number of kaons of each type with the total number of kaons produced in each simulation with a different enhancement factor is presented in Figure 5.2. The fraction is;

$$\text{Fraction} = \frac{\text{No of kaons of one type}}{\text{Total no of kaons}}$$

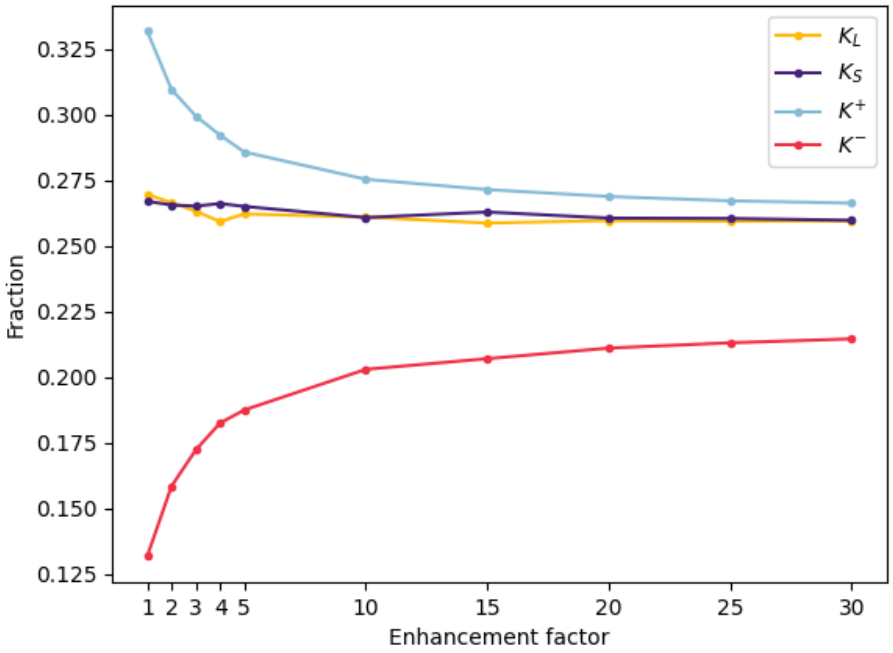

Figure 5.2: Fraction of kaons in simulations using UpKaons.

The fractions of the neutral kaons are stable with the increase of the enhancement factor. The fractions of the charged kaons change rapidly from enhancement factor 1 to then level out. This could be due to the difference in primary and secondary reactions. In the low range of the enhancement factors, the fraction of secondary reactions is not insignificant, and it is much more common with a K^+ than a K^-. A reason for this could derive from the difference in energies for the primary and the secondary reactions and the quark content of the different kaons. A K^- contains a strange quark (s) and an antiquark ($\bar{u}$), a K^+ contains a quark (u) and an antiquark ($\bar{s}$). The u-quarks are easy to get (present in both protons and neutrons for instance), but the $\bar{u}$ needs to be accessed from the quarks sea and this requires more energy. So, for a low enhancement factor, where the fraction of lower energy secondary productions is higher, it is more difficult to get $\bar{u}$ from the quark sea. So, with lower energy, it is more difficult to get $\bar{u}$-quarks, which in turn affects the production of K^-. This difference is not apparent in the neutral kaons since they have the same quark content.

Although there is a difference in the kaon fraction for the charged kaons, it should not introduce difficulty in the vetoing process since the charged kaons are vetoed in the same way and have the same lifetime.

5.3 Boost factor

The main feature of the changes in the UpKaons Geant4 simulation is that a boost of the kaon production is introduced. The comparison of the input enhancement factor to the calculated boost factor is presented in Table 5.2 and Figure 5.3. The enhancement factor is the input parameter that is set in the configuration. The calculated boost factor is the observed increase in kaon production. The calculations were done both comparing kaon events and the total number of kaons produced in the simulated samples. The formula used was;

$$\text{Boost factor} = \frac{\text{biased events}}{\text{unbiased events}} \times \frac{\text{unbiased started events}}{\text{biased started events}}$$

When comparing the number of kaons, events were replaced by the number of kaons.

Enhancement factor	Events started	Total no. of kaon events	Total no. of kaons	Boost factor based on events	Boost factor based on number of kaons
1	96×10^6	20124	27162	1	1
2	95×10^6	26671	38848	1.312	1.445
3	98×10^6	34549	52296	1.682	1.886
4	98×10^6	41487	64324	2.019	2.320
5	98×10^6	48017	75592	2.337	2.726
10	94×10^6	77735	128146	3.945	4.818
15	94×10^6	109341	182917	5.548	6.878
20	99×10^6	147764	249770	7.120	8.917
25	99×10^6	177791	302085	8.567	10.78
30	93×10^6	198463	338810	10.18	12.88

Table 5.2: Calculated boost factors for input enhancement factors 1-30.

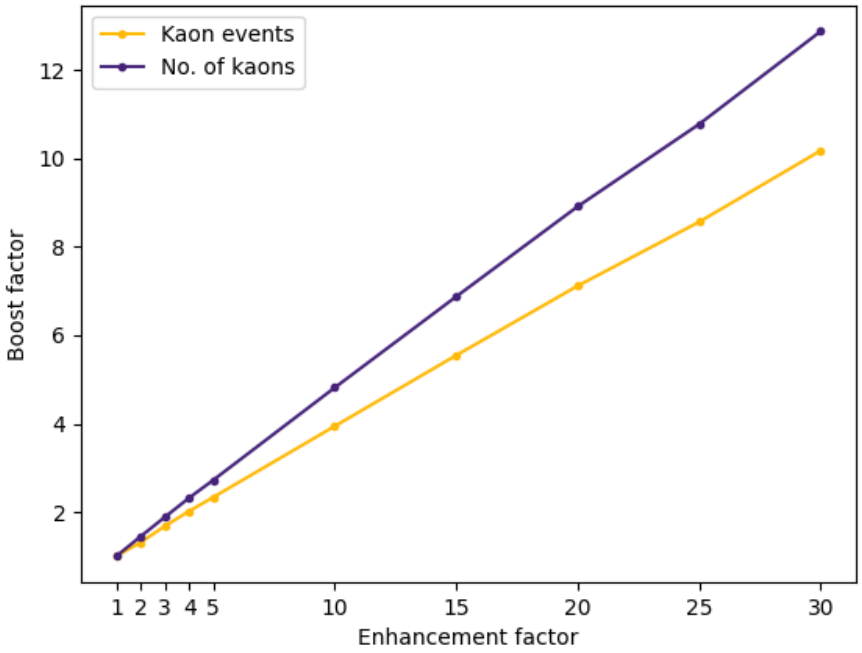

Figure 5.3: Comparison of calculated boost factors.

The calculated boost in production does not agree with the enhancement factors in the simulations. That is, adding an enhancement factor of 25 will not increase the number of kaons by a factor of 25. There is a linearity for both the boost factor calculated with the number of kaon events and for the boost for the total number of kaons. Also, the boost factor does not converge to some number but diverges, which is to be expected.

5.4 Energy

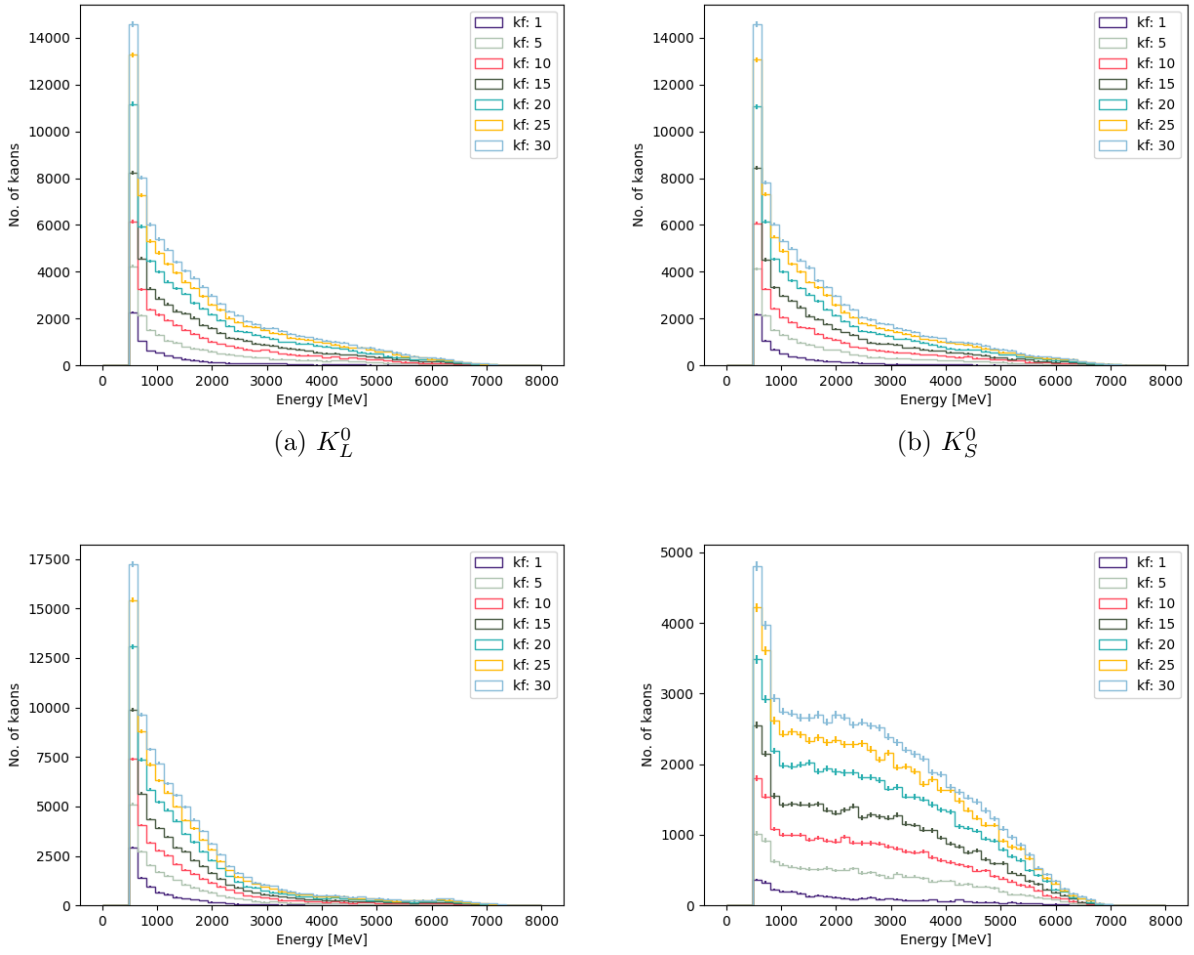

(a) K_L^0

(b) K_S^0

(c) K^+

(d) K^-

Figure 5.4: Histogram of energy distribution for K_L^0, K_S^0, K^+ and K^-.

The plots in Figure 5.4 show that the energy of the kaons increases slightly with an increase of enhancement factor. This is true for all four kaon types. The data in Figure 5.4 is not normalized, therefore there is a difference in the number of kaons for each enhancement factor. By normalizing the data and changing the y-axis scale to log scale it becomes easier to compare the distributions and analyze the tails.

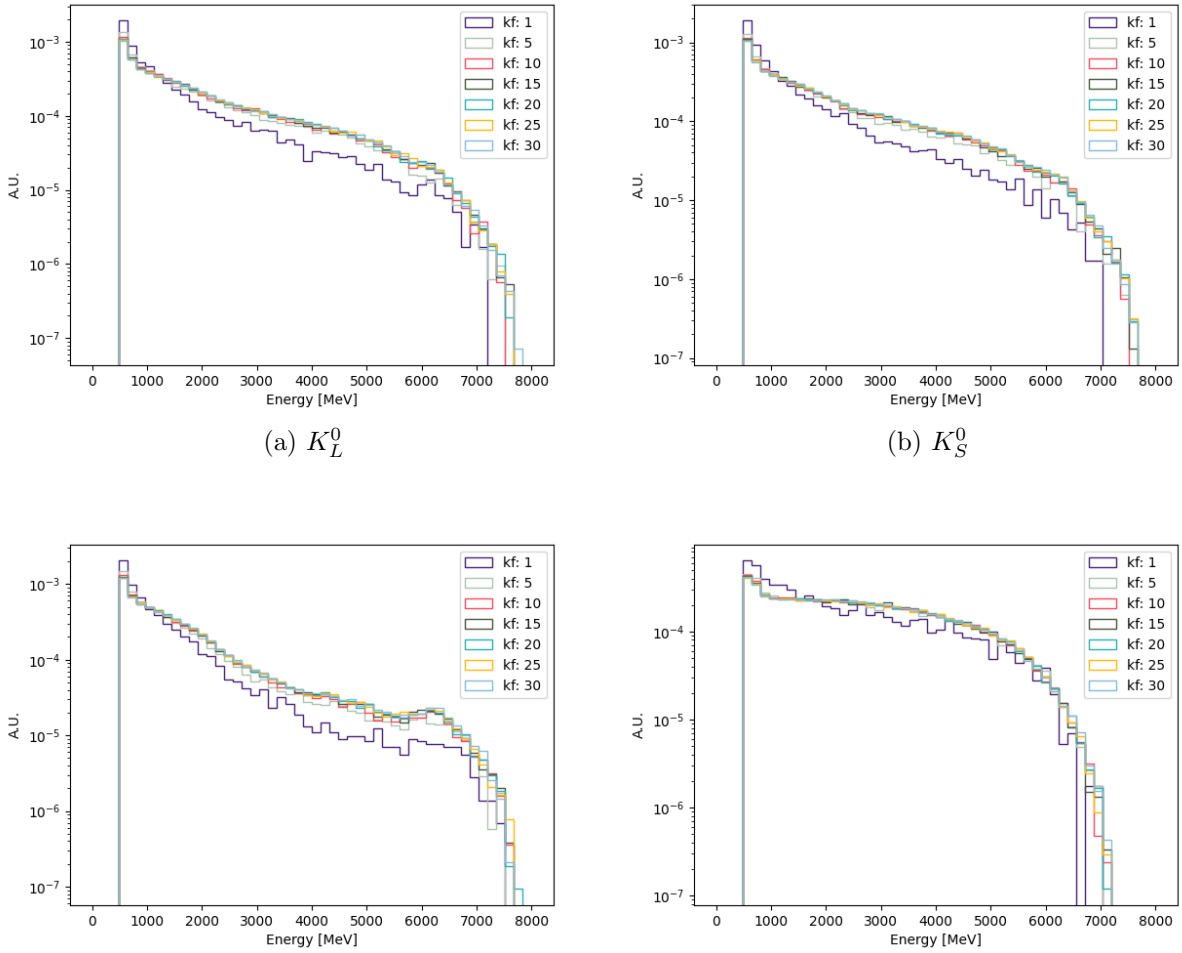

(a) K_L^0 (b) K_S^0

(c) K^+ (d) K^-

Figure 5.5: Normalized energy distribution for enhancement factors 1-30.

Analyzing the energy plots in Figure 5.5, the energy distribution is slightly different for the samples that have a larger enhancement factor than 1. The shape is different when moving from enhancement factor 1 to enhancement factor 5. Though for enhancement factor 5 to enhancement factor 30 the shapes are very similar. Also, the energy is increasing with increasing enhancement factors. These effects could be explained by the difference in primary versus secondary produced kaons.

5.5 Angle θ

The angle θ indicates the deviation from the incoming beam direction, the z-direction. The parameter ranges from 0 to π and kaons with a value greater than $\pi/2$ are going backward in the detector.

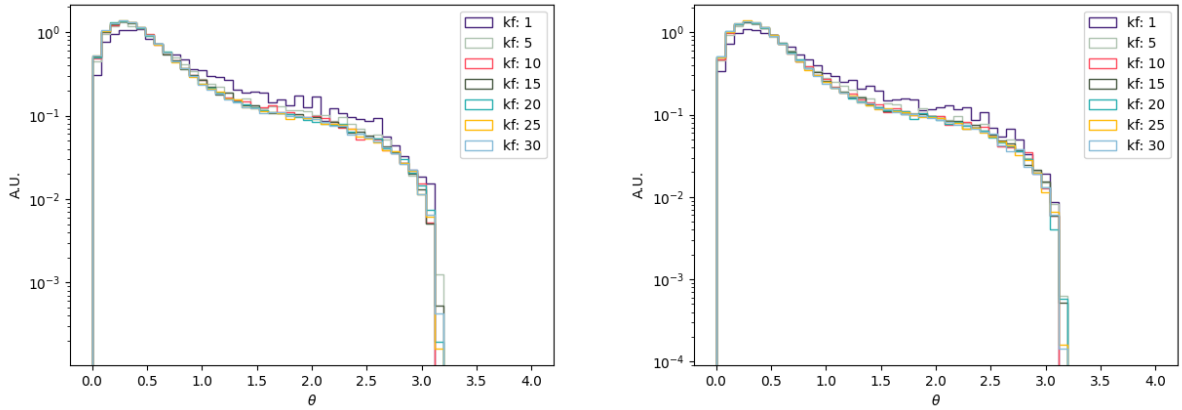

(a) K_L^0 (b) K_S^0

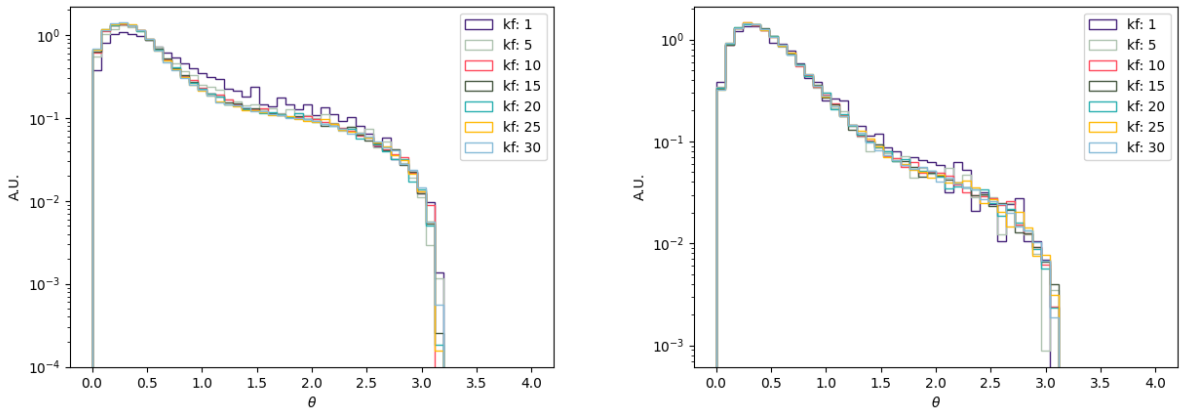

(c) K^+ (d) K^-

Figure 5.6: Angle θ away from the beam direction for K_L^0, K_S^0, K^+ and K^-. Angles larger $\pi/2$ are directed backward in the detector.

For all kaon types, most of the kaons have a small angle away from the beam direction. There is a difference between enhancement factor 1 and the higher enhancement factors which do not deviate from each other. Again, this could be due to the difference in primary and secondary produced kaons.

5.6 Location of production and end point

To further study the kaons produced in the simulations, plots were made of the production location, endpoint, and length of the kaons path through the detector. The production location is the z-coordinate of the production vertex, the endpoint is where the kaon is destroyed or leaves the detector, also in the z-direction. The length is calculated as the distance between the production vertex and the endpoint, in three dimensions.

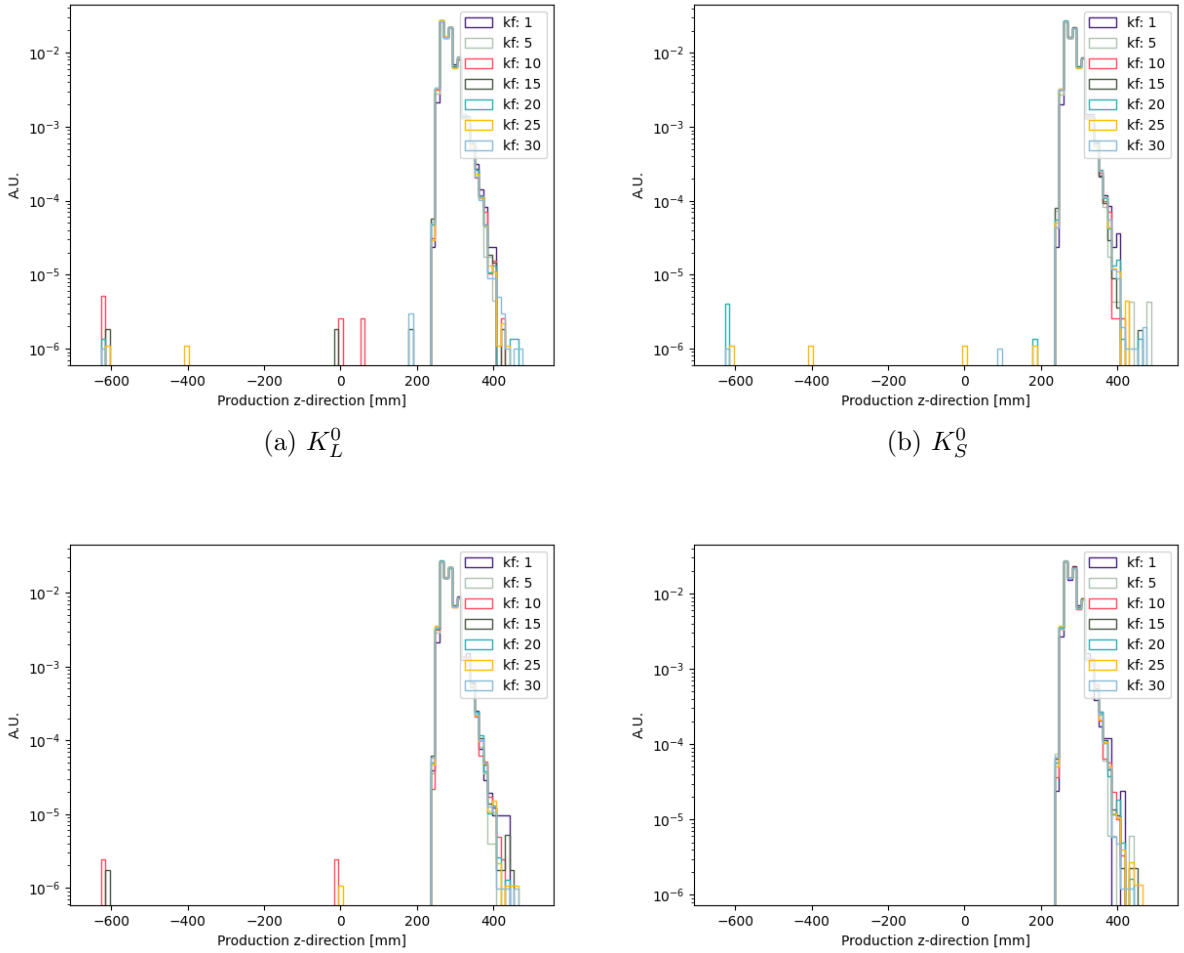

(a) K_L^0 (b) K_S^0

(c) K^+ (d) K^-

Figure 5.7: Production location in the z-direction for K_L^0, K_S^0, K^+ and K^-. 0 mm corresponds to the target and 240 mm to the front end of the ECal.

Apart from a few kaons produced at the target and other locations in the detector, most of the production happens around 240 mm and after and the distribution does not differ much between the kaon types. The production location matches the front of the ECal as expected.

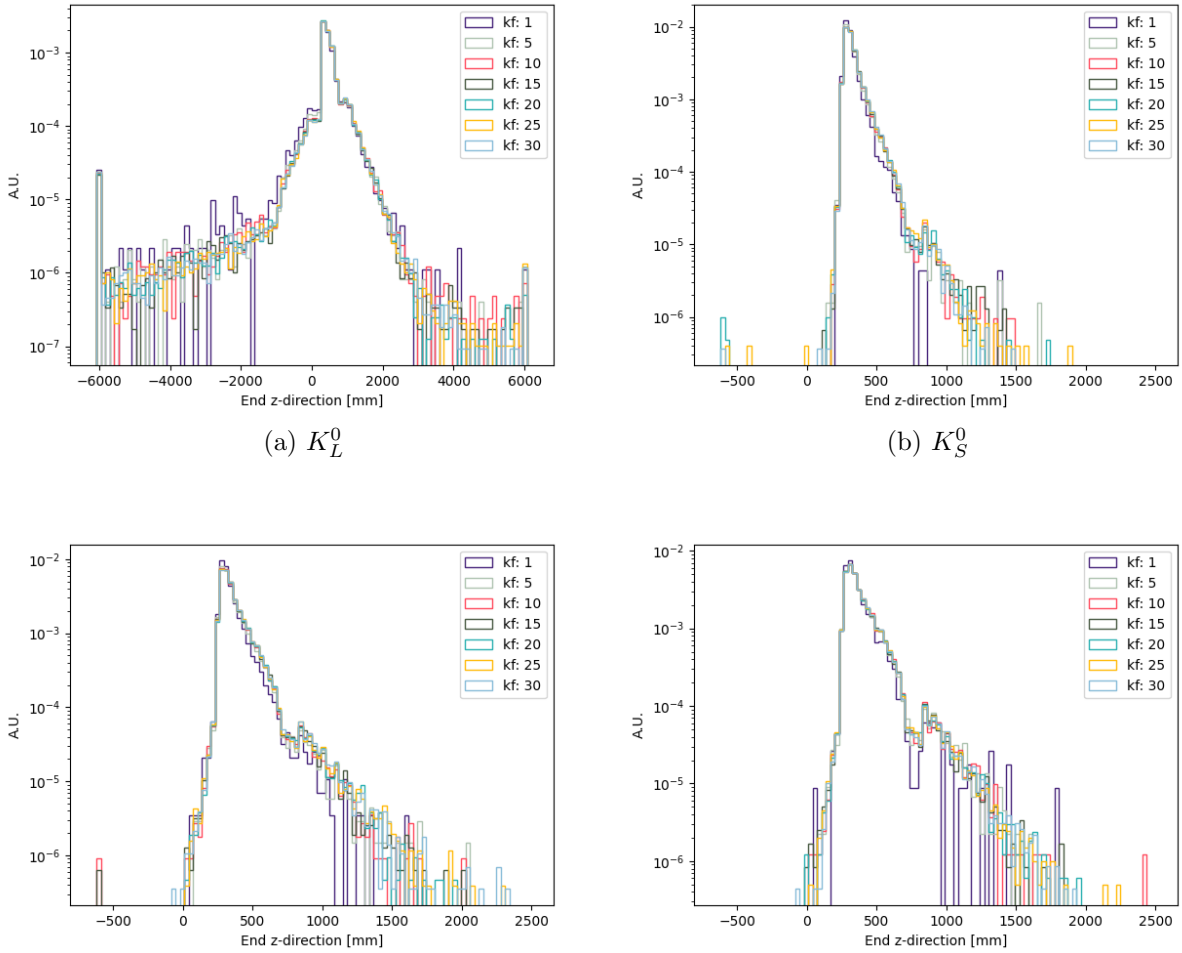

(a) K_L^0 (b) K_S^0

(c) K^+ (d) K^-

Figure 5.8: End location in the z-direction for K_L^0, K_S^0, K^+ and K^-. 240 mm corresponds to the front of the ECal. The detector volume in the simulations does not extend over 6000 mm, indicating that this is where some K_L^0 leaves the detector without being destroyed.

The peaks of the endpoints in Figure 5.8 are all a small distance away from the front ECal, where most of the kaons are produced. There also seems to be a slight difference between enhancement factor 1 and the other factors. Some K_L^0 particles leave the detector before they decay into other particles. Comparing the neutral kaons, the endpoint has a larger magnitude for the K_L^0 than for the K_S^0, as expected due to their different lifetimes. The charged kaons, K^+ and K^-, show a similar distribution, which is expected since they have the same lifetime.

There is also a dip in the curves around 600-800 mm from the target at 0 mm. This dip is present for all kaon types. In Figure 5.9, showing the length of the kaons through the detector, the dip is even more noticeable. The location of the dip coincides with a gap between the ECal and the HCal in the definition of the detector version that is used in the simulations. By looking at the detector specifications in [9], there is a gap of 15 cm between

the ECal and the back HCal. In this gap there is no material, hence nothing for particles to interact with which creates a dent in the endpoint and the length plots.

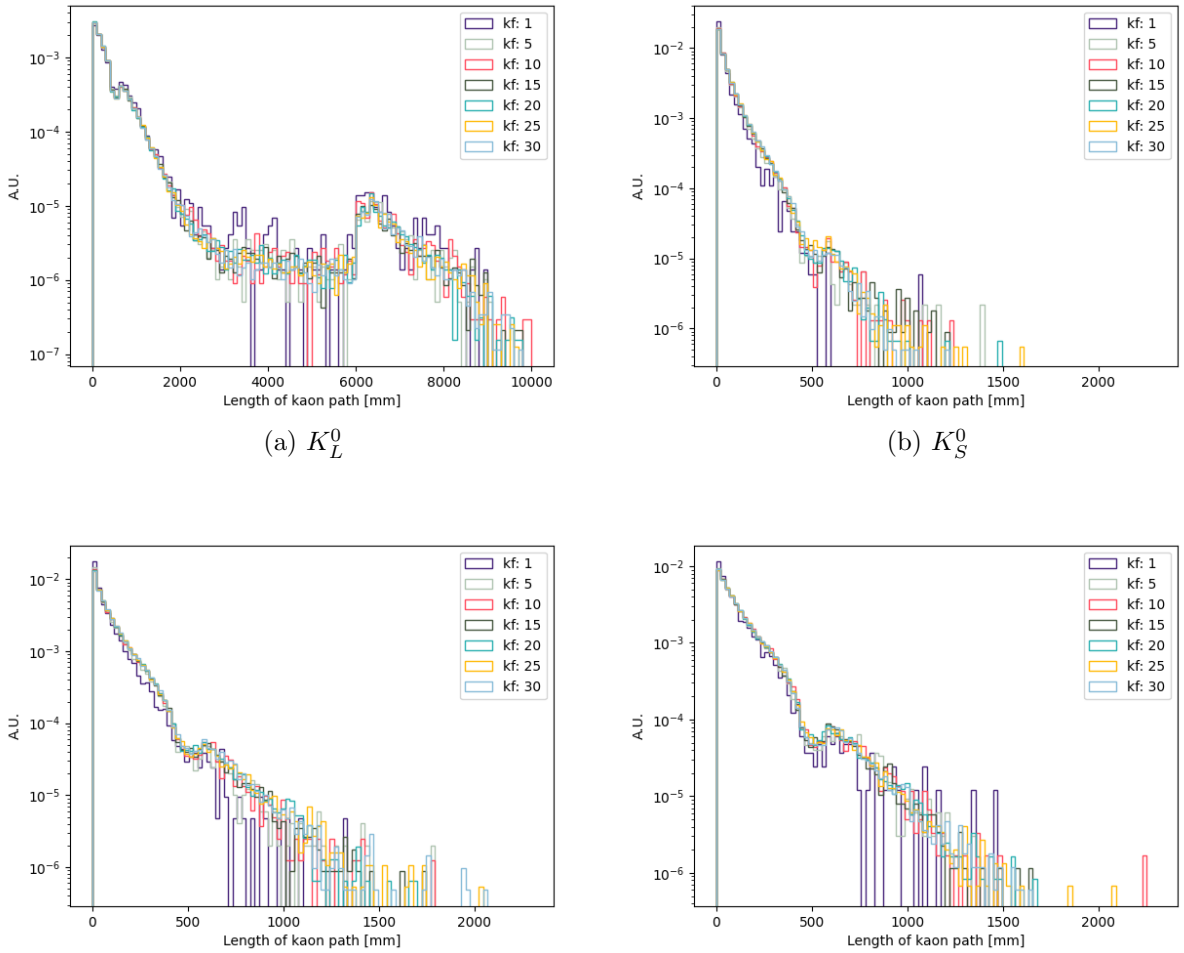

(a) K_L^0 (b) K_S^0

(c) K^+ (d) K^-

Figure 5.9: Length of kaon tracks in the LDMX detector for K_L^0, K_S^0, K^+ and K^-.

Figure 5.9 also shows that the decay length of the kaons changes with an added boost factor, and the kaons travel further. Since there is an increase in the energy of the kaons due to the difference in the primary versus secondary production this is expected. However, the biasing itself makes the charged kaons travel a shorter distance since the biasing factor results in an increase in the number of early leptonic decays. But as seen in Figure 5.9, the increase in average energy due to the difference in primary and secondary production of kaons seems to have a larger impact on the length of the kaon tracks.

5.7 Process type

In the simulation, the process type which the particle originates from is recorded. Most of the kaons are expected to come from pn reactions in the simulation. Plotting the process type confirms this, see Figure 5.10. Most of the kaons originate from a pn reaction, corresponding to process type 9 in the plots. Process type 0 is labeled as an unknown process and 4 is an electronuclear reaction. Other possibilities for processes are electron bremsstrahlung, dark bremsstrahlung, and gamma-to-muon-pair to mention a few.

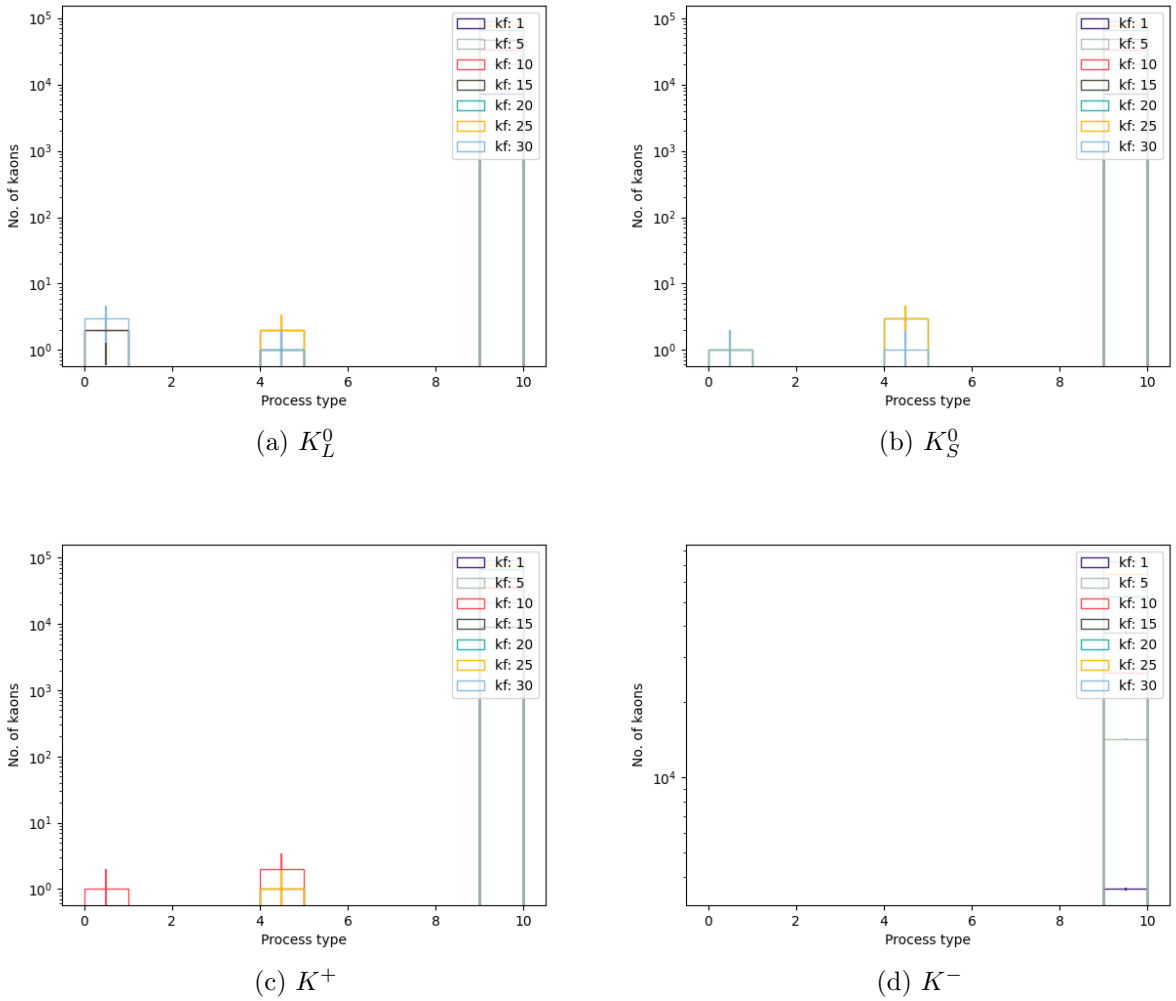

(a) K_L^0 (b) K_S^0

(c) K^+ (d) K^-

Figure 5.10: Process type the kaon is originating from for K_L^0, K_S^0, K^+ and K^-. Process type 9 is a photonuclear reaction, 4 is an electronuclear reaction and 0 is an unknown process.

By analyzing a 2d plot comparing the process type with the production location it becomes clear that the kaons that were produced at unexpected positions in front of the target in Figure 5.7 do not come from a pn reaction but unknown processes or electronuclear processes. This can be seen in Figure 5.11.

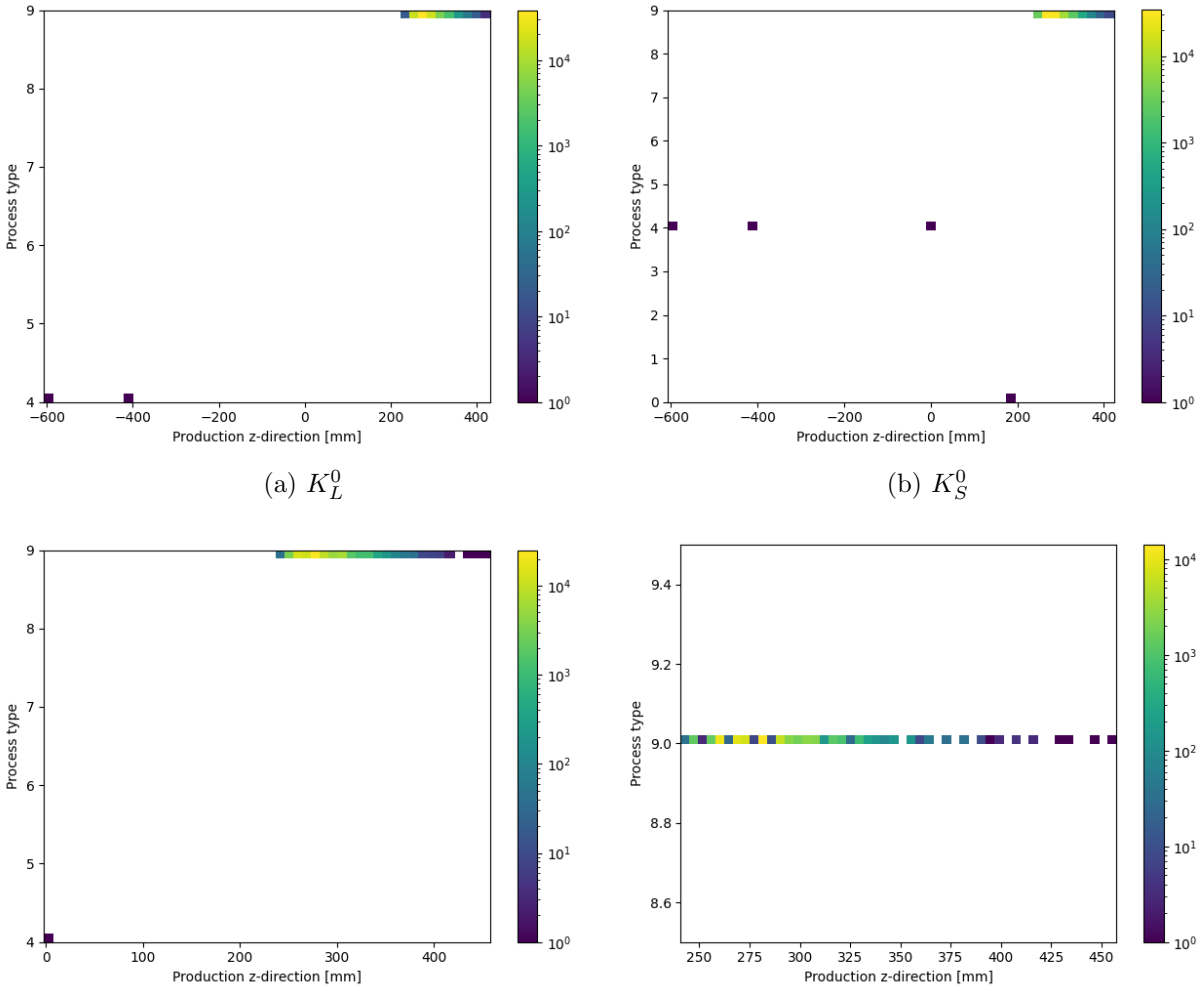

(a) K_L^0 (b) K_S^0

(c) K^+ (d) K^-

Figure 5.11: Production location vs Process type for K_L^0, K_S^0, K^+ and K^-, all with enhancement factor 25

5.8 2d plots

To study the kaons further, a series of 2d plots were produced, as this should give further information about the characteristics of the kaons. Since the previous plots did not show a significant difference in the curves for enhancement factor 5-30, the following plots all show simulated data with enhancement factor 25.

5.8.1 Energy versus angle

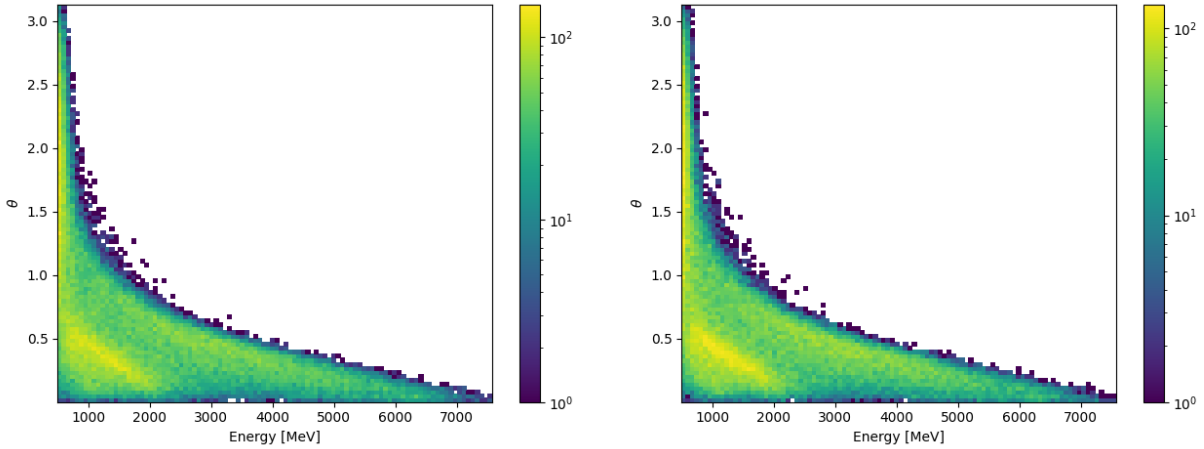

(a) K_L^0

(b) K_S^0

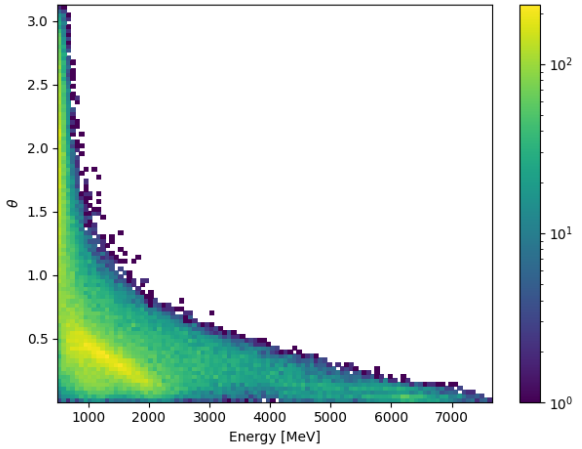

(c) K^+

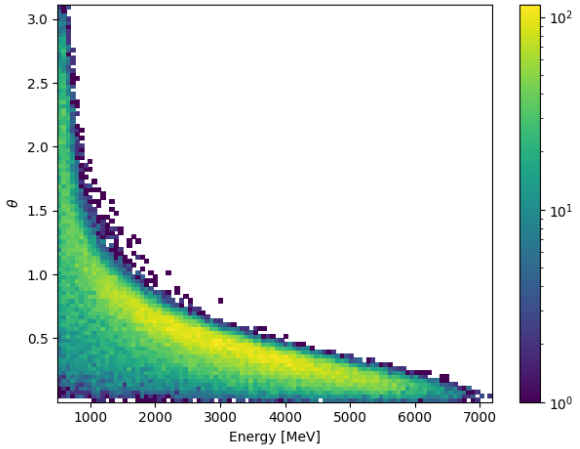

(d) K^-

Figure 5.12: Energy versus angle θ for K_L^0, K_S^0, K^+ and K^-, enhancement factor 25.

For all kaon types, the particles with the largest angle have the lowest energy, and the most energetic particles are in the forward direction. The distributions are very similar for K_L^0, K_S^0 and K^+ but for K^- there is difference for the energy. This difference can also be seen in the energy plots in Figure 5.5.

5.8.2 Production location versus length

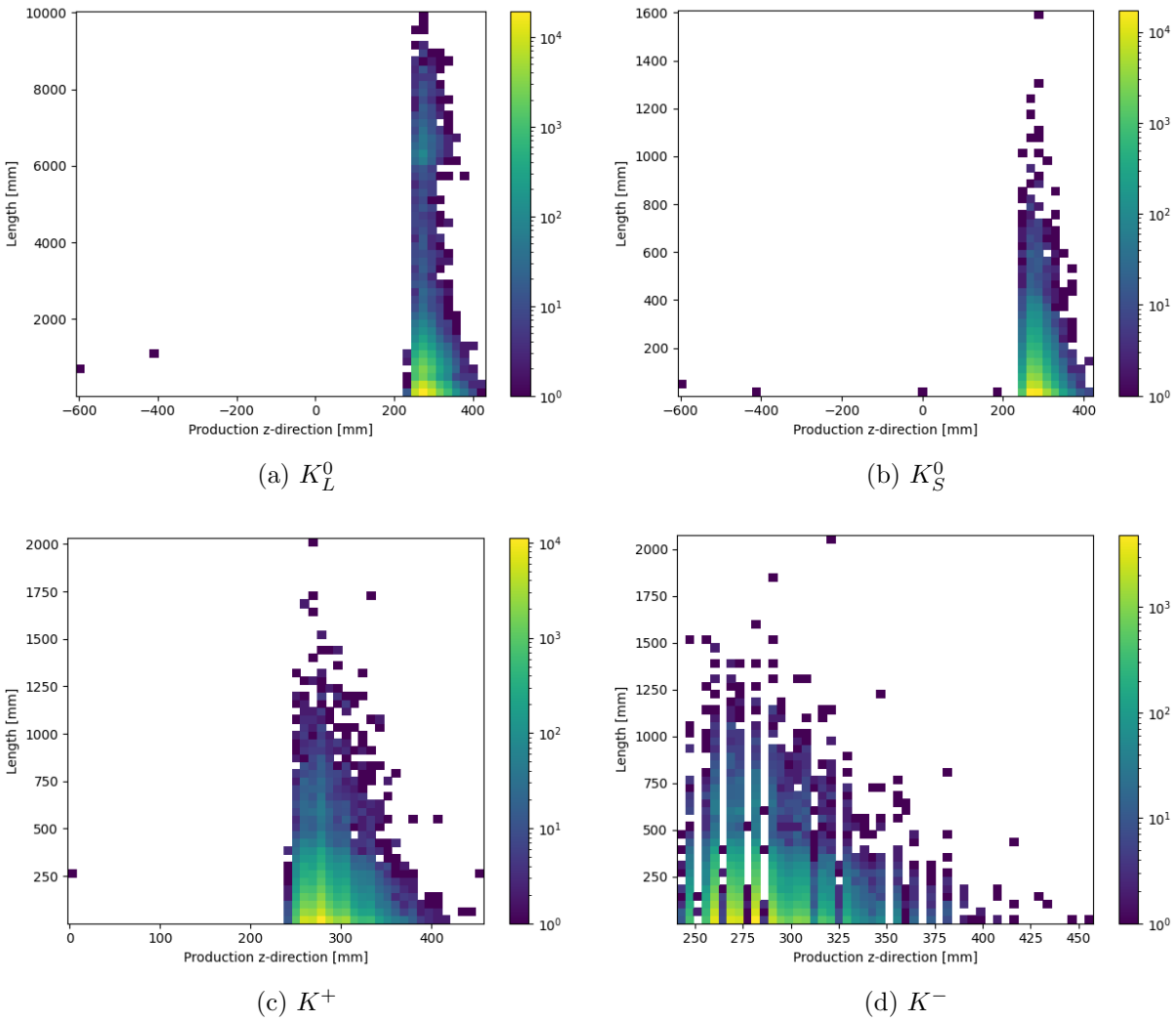

(a) K_L^0

(b) K_S^0

(c) K^+

(d) K^-

Figure 5.13: Production location in the z-direction versus the length for K_L^0, K_S^0, K^+ and K^-, enhancement factor 25.

For K_L^0, K_S^0 and K^+, the kaons produced in the front of the ECal are the ones that travel the longest in the detector, and it is also very common that the length of the kaon tracks is short. It is also noticeable that in the K^- plot, the layer structure of the ECal is also visible since it is more zoomed in than for the other kaons. There is a larger probability that the production happens in some layers.

5.8.3 Endpoint versus angle θ

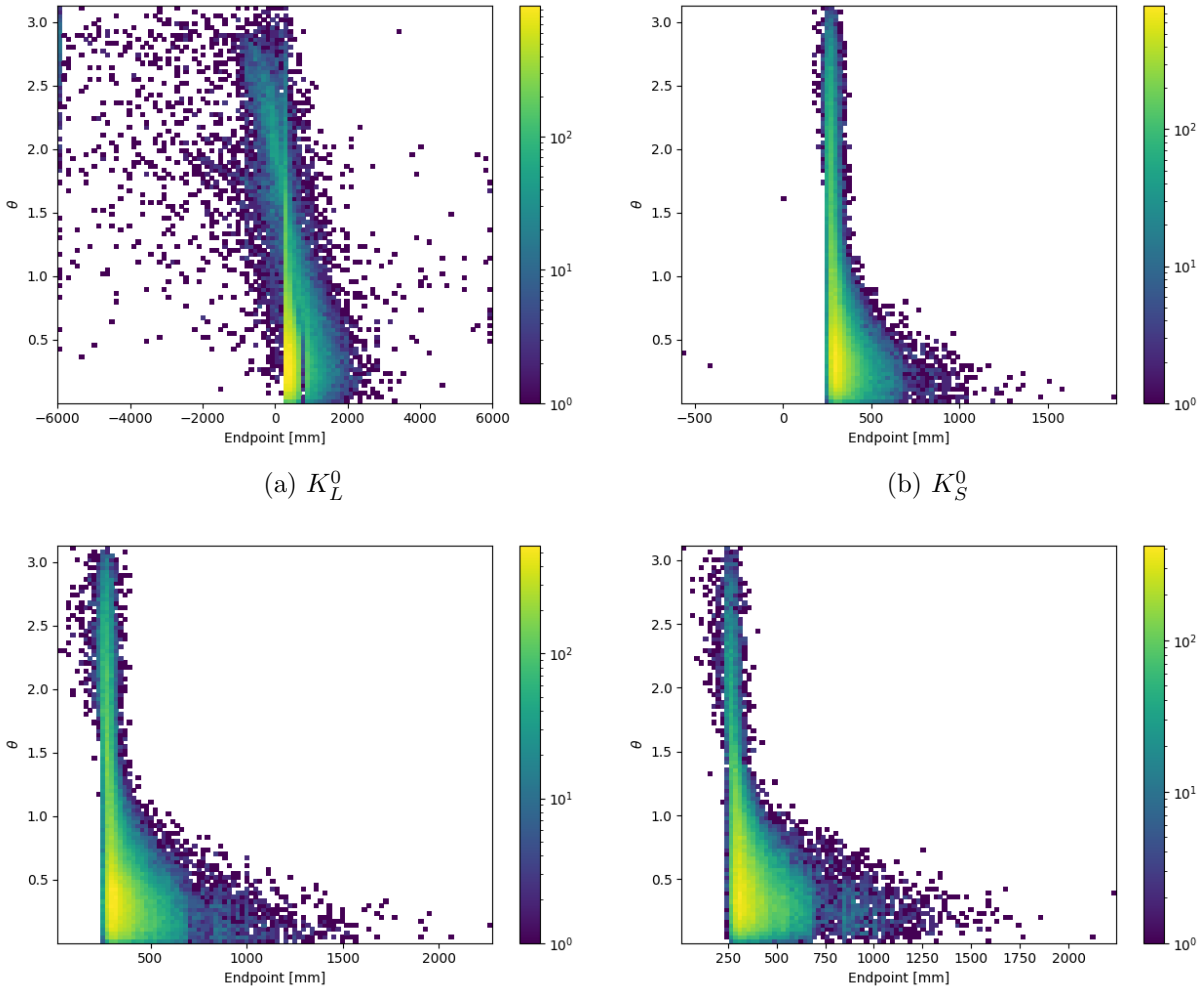

(a) K_L^0

(b) K_S^0

(c) K^+

(d) K^-

Figure 5.14: End location in the z-direction versus angle θ for for K_L^0, K_S^0, K^+ and K^-, enhancement factor 25

When the angle is above $\pi/2$ it is directed upstream in the detector. Hence the endpoint is more likely to be before the front of the ECal, this is especially visible when looking at K_L^0 since this kaon has the longest lifetime before it decays, and therefore it has longer tracks.

5.8.4 Angle θ versus length

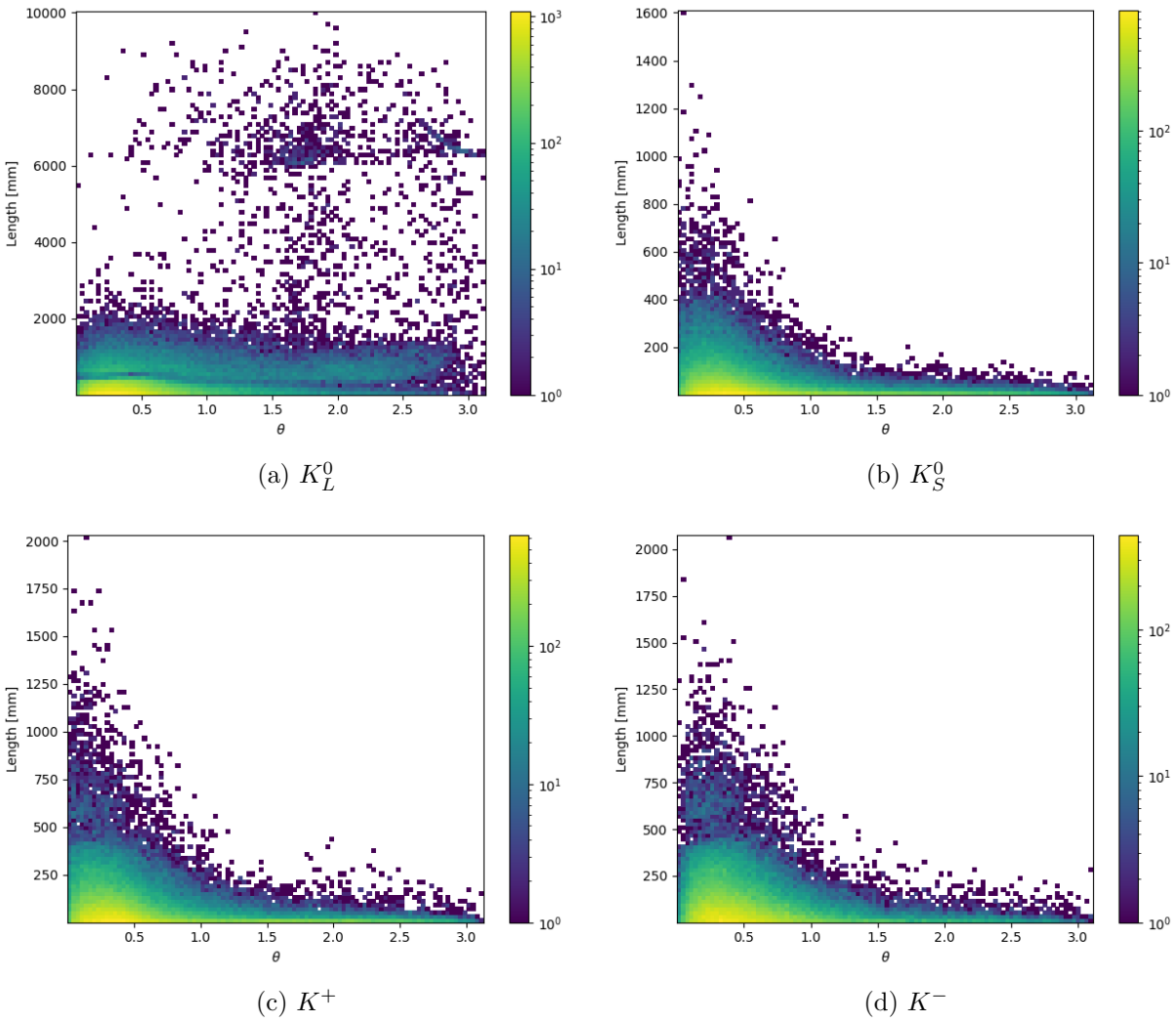

(a) K_L^0

(b) K_S^0

(c) K^+

(d) K^-

Figure 5.15: Angle θ vs the length for for K_L^0, K_S^0, K^+ and K^-, enhancement factor 25.

Studying Figure 5.15a, most of the K_L^0 have a small angle, but particles with all angle theta can travel a long distance. There is a blue ribbon in the 2d plot corresponding to the dip that was present in Figure 5.8a and 5.9a showing the endpoint and the length of K_L^0. For the other kaon types in Figure 5.15 the particles with a larger angle away from the beam direction correspond to a small distance.

5.8.5 Energy versus length

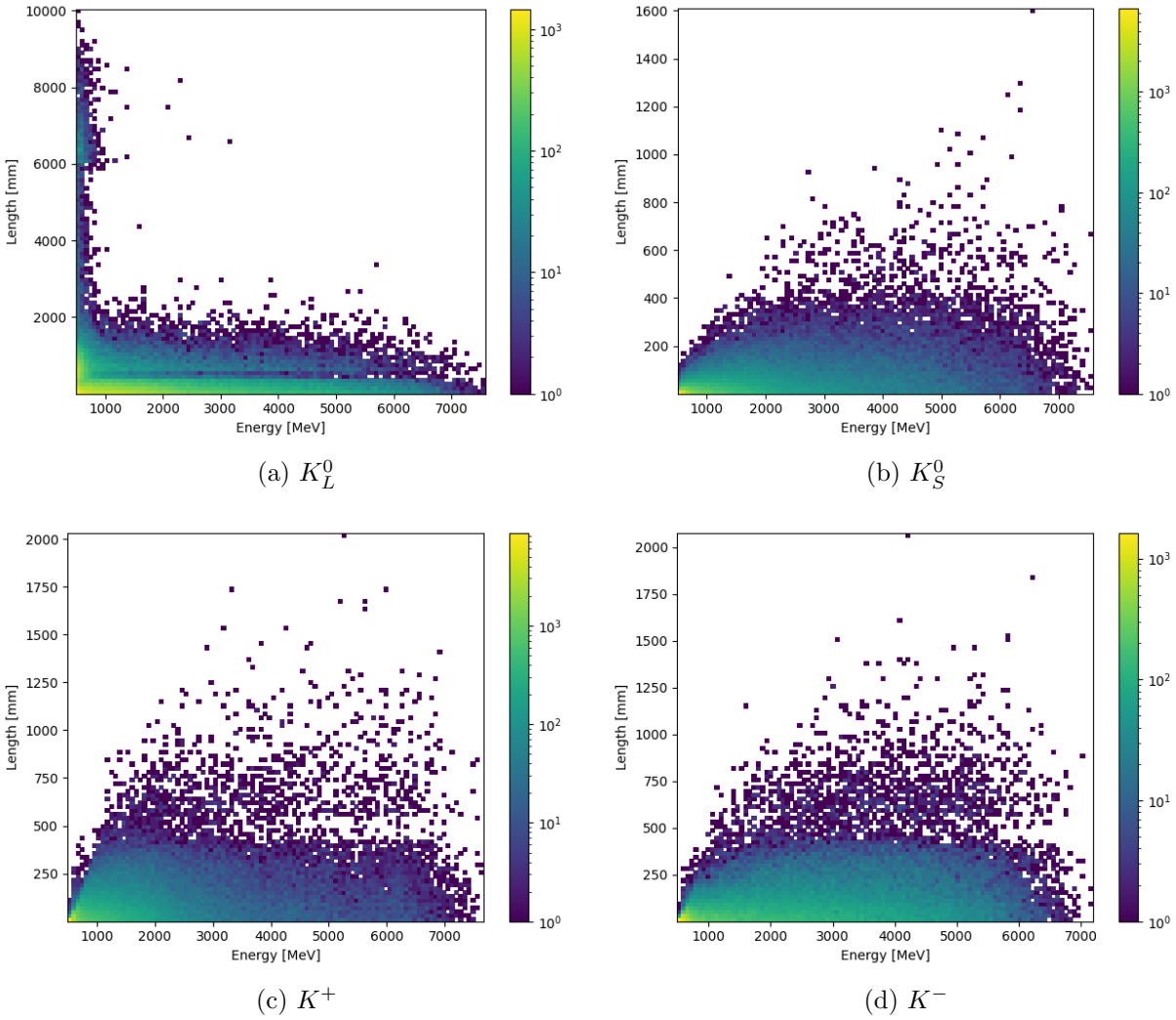

(a) K_L^0

(b) K_S^0

(c) K^+

(d) K^-

Figure 5.16: Energy versus length for for K_L^0, K_S^0, K^+ and K^-, enhancement factor 25.

When plotting the Energy versus the length of the kaon tracks there is not a huge difference between the K_S^0, K^+, and K^-. However, for the K_L^0, it is the particles with the lowest energy that have the longest tracks.

Also here the dip that was present in Figure 5.8 and 5.9 are visible for all kaons, but especially for K_L^0 where it is seen as a horizontal line.

Chapter 6

Conclusion

After analyzing all plots carefully and ironing out all the question marks on the way, there seems to be no unphysical behavior being added when boosting the kaon production.
In all studied variables, there is a difference in the distribution from enhancement factor 1 to higher enhancement factors but almost no difference between enhancement factors 5-30. The main effect of the boost is seen in the energy spectra, though small changes in the event topologies can be seen in all plot variables. This difference could be due to the production boost being applied only to the primary production of kaons.

The differences seen when adding an enhancement factor needs to be considered. For example, if the ECal BDT is trained on boosted kaons, then it would be trained on an energy that is slightly too high. This indicates that a correction for this needs to be implemented if the ECal BDT is to be trained on an enhanced kaon sample. The shape is probably slightly distorted since the enhancement factor is just affecting the primary production, which in general has higher energy.

If the difference seen in the event topologies is due to the difference between primary production and secondary production and the fact that the boost factor only affects the primary productions then there are two suggestions to correct this. Either one could reweight the result and correct for the differences "forcing" the distribution to look like the unbiased samples. Another suggestion is to implement a boost factor on the secondary produced kaons as well.

It was found that the decay lengths are increasing with an added boost factor. A longer decay length might make it easier to separate the kaon background from a dark matter signal. If a reweighting is done to correct for the difference seen in the energy distributions this might change back to the initial lengths.

Another conclusion that can be drawn from the analysis is that there is no need to produce samples with a lot of different enhancement factors in future studies. Once the kaon production is boosted above enhancement factor 1 there is not much difference between the distribution curves.

There was a dip in the endpoint and length plots that was puzzling at first. Though when studying the detector geometry carefully it was noticed that there is a gap of 15 cm between the ECal and the back HCal in the detector version that was used in the simulations. In this section, there is no material for particles to interact with, hence the dip.

6.1 Summary

By simulating and analyzing data with a boosted kaon production using a modified Geant4 simulation and the software framework for LDMX, a study has been conducted on the effects of the boost. The simulated samples show no unphysical behavior but there are some differences in the event topologies that need to be taken into consideration if a boosted sample is to be used for training the ECal BDT. Some differences that are seen, such as the decay length of the kaons, might improve the possibility to separate the kaon background from signal events.

The differences that are seen in the boosted samples compared to the ones with enhancement factor 1 could be due to the fact that the boost only affects the primary production of kaons and not the secondary production. At this point, this is a plausible theory but needs to be studied more to be able to be verified.

Some events that pass the filtering have no kaons in them. The kaon filter that is added should make sure that there is a kaon somewhere in the products of a pn reaction, if not, the event would be discarded. The reason for the events without kaons is not known yet but it is currently under investigation within the LDMX collaboration.

In some events, there is more than one kaon per event. The total maximum number of kaons per event has not been tested but for the individual kaon types the maximum number of kaons per event is 4. Without studying the kaons more carefully in such an event there is no general conclusion to be drawn from this. A check that could be made is to see if the kaons in one event all originate from the same pn reaction or if there are more pn reactions in one event. This could be done by comparing if the kaons originate from a pn reaction that was initialized by the same particle.

Bibliography

[1] Åkesson T, Blinov N, Bryngemark L, Colegrove O, Collura G, Dukes C, et al. A high efficiency photon veto for the Light Dark Matter eXperiment. Journal of High Energy Physics. 2020;2020(4):1-35.

[2] Åkesson T, Blinov N, Brand-Baugher L, Bravo C, Bryngemark LK, Butti P, et al. Current Status and Future Prospects for the Light Dark Matter eXperiment. arXiv preprint arXiv:220308192. 2022.

[3] Åkesson T, Berlin A, Blinov N, Colegrove O, Collura G, Dutta V, et al. Light dark matter eXperiment (LDMX). arXiv preprint arXiv:180805219. 2018.

[4] CERN-Science, Dark matter mass in the Universe;. Accessed: 2023-01-10. https://home.cern/science/physics/dark-matter.

[5] Perkins DH, Perkins DH. Introduction to high energy physics. CAMBRIDGE university press; 2000.

[6] Povh B, Rith K, Scholz C, Zetsche F, Rodejohann W. Particles and nuclei. An Introduction to the Physical Concepts, Berlin and Heidelberg: Springer-Verlag (Italian Translation:(1998), Particelle e nuclei Un'introduzione ai concetti sici, Torino: Bollati Boringhieri editore). 1995.

[7] Griffiths D. Introduction to elementary particles. John Wiley & Sons; 2020.

[8] Workman RL, Others. PDG - Review of Particle Physics. PTEP. 2022;2022:083C01.

[9] ldmx-sw;. Accessed: 2023-01-10. https://github.com/LDMX-Software.

[10] Agostinelli S, Allison J, Amako Ka, Apostolakis J, Araujo H, Arce P, et al. GEANT4—a simulation toolkit. Nuclear instruments and methods in physics research section A: Accelerators, Spectrometers, Detectors and Associated Equipment. 2003;506(3):250-303.

[11] LUNARC - center for scientific and technical computing at Lund University;. Accessed: 2023-01-10. https://www.lunarc.lu.se.

[12] ROOT;. Accessed: 2023-01-11. https://root.cern/.

[13] Python;. Accessed: 2023-01-11. https://www.python.org/.

[14] Matplotlib;. Accessed: 2023-01-11. https://matplotlib.org/.

Appendix A

Configuration file

```
#Run this config file using ldmx-sw with UpKaons branch to simulate 8 Gev
#electron beam producing a sample with enhanced kaon production, also use
#modified Biasing/python/ecal.py to turn on kaon filtering.

from LDMX.Framework import ldmxcfg

p=ldmxcfg.Process("test")
p.run = 25074 #Set Individual run number for each run
kaon_factor = 25 #Enhancement factor, default is 25, can be set between 0
                                    and 30

from LDMX.SimCore import bias_operators
from LDMX.SimCore import simulator
from LDMX.Ecal import EcalGeometry
from LDMX.Hcal import HcalGeometry
import LDMX.Ecal.ecal_hardcoded_conditions as ecal_conditions
import LDMX.Hcal.hcal_hardcoded_conditions as hcal_conditions

from LDMX.Biasing import ecal  #target
from LDMX.SimCore import generators
#Set detector version, change from 4 to 8 to generate an 8 GeV electron
                                    beam.
mysim = ecal.kaon_pn('ldmx-det-v13', generators.
                                    single_8gev_e_upstream_tagger())
mysim.description = "ECal Kaon Test Simulation, 8GeV"
print(mysim)

import LDMX.Ecal.digi as ecal_digi
import LDMX.Hcal.digi as hcal_digi
import LDMX.Ecal.vetos as ecal_vetos
import LDMX.Hcal.hcal as hcal_py
from LDMX.Recon.simpleTrigger import simpleTrigger
from LDMX.Recon.electronCounter import ElectronCounter #to allow for multi
                                    -e, electron counter needed

from LDMX.TrigScint.trigScint import TrigScintDigiProducer
from LDMX.TrigScint.trigScint import TrigScintClusterProducer
```

```
from LDMX.TrigScint.trigScint import trigScintTrack

tsDigisUp   = TrigScintDigiProducer.up()
tsDigisTag  = TrigScintDigiProducer.tagger()
tsDigisDown = TrigScintDigiProducer.down()

#these lines required for trigger skimming
eCount = ElectronCounter(1, "ElectronCounter") #first argument is number
                                    of electrons in simulation
eCount.use_simulated_electron_number = True
simpleTrigger.end_layer = 20
simpleTrigger.start_layer = 0 #default is 1, force to include first layer
#these two lines turn on trigger skimming
#p.skimDefaultIsDrop()
#p.skimConsider(simpleTrigger.instanceName)p.run = 1p.run = 1

p.sequence=[ mysim,
        ecal_digi.EcalDigiProducer(),
        ecal_digi.EcalRecProducer(),
        ecal_vetos.EcalVetoProcessor(),
        hcal_digi.HcalDigiProducer(),
        hcal_digi.HcalRecProducer(),
        hcal_py.HcalVetoProcessor(),
        tsDigisUp, tsDigisTag, tsDigisDown,
        #trigScintTrack,
        eCount,
        simpleTrigger
        ]

p.outputFiles=["output/kaon_enhancement_{}/upKaons8_testprod_{}_run{}.root
                                    ".format(kaon_factor,kaon_factor, p.
                                    run)]

p.maxTriesPerEvent = 1 #max number of attempts to create an event before
                                    moving on, default is 1

p.maxEvents = 1000000 #events started, reduce this number if testing

p.logFrequency = 10000 #Set to 1 when de-bugging
```

Appendix B

Biasing/python/ecal.py

```
    """Example configurations for producing biased interactions in the
                                        ECal.

    Example
    -------

        from LDMX.Biasing import ecal
"""

from LDMX.SimCore import simulator
from LDMX.SimCore import generators
from LDMX.SimCore import bias_operators
from LDMX.Biasing import filters
from LDMX.Biasing import util
from LDMX.Biasing import include as includeBiasing
from LDMX.Biasing import particle_filter

def photo_nuclear( detector, generator ) :
    """Example configuration for producing photo-nuclear reactions in the
                                        ECal.

    In this particular example, 4 GeV electrons are fired upstream of the
    tagger tracker.  The TargetBremFilter filters out all events that don'
                                        t
    produced a brem in the target with an energy greater than 2.5 GeV.
                                        The
    brems are allowed to propagate to the ECal at which point they are
    checked by the EcalProcessFilter.  Only events that see the brem
                                        photon
    undergo a photo-nucler reaction in the ECal are kept.

    Parameters
    ----------

    detector : str
        Path to the detector
    generator : PrimaryGenerator
        generator to use
```

```
    Returns
    -------
    Instance of the simulator configured for ECal photo-nuclear.

    Example
    -------

        ecal_pn_sim = ecal.photo_nuclear('ldmx-det-v12')

    """


    # Instantiate the simulator.
    sim = simulator.simulator("photo-nuclear")

    # Set the path to the detector to use.
    #   the second parameter says we want to include scoring planes
    sim.setDetector( detector , True )

    # Set run parameters
    #sim.runNumber = 0
    sim.description = "ECal photo-nuclear, xsec bias 550"
    sim.beamSpotSmear = [20., 80., 0.] #mm

    sim.generators.append( generator )

    # Enable and configure the biasing
    #   In order to conform to older samples,
    #   we can only attach to some of the volumes in the ecal
    #   so we ask for this operator to be attached to the 'old_ecal'
    #  biasing factors are 450., 2500. for 4GeV, 550., 4500. for 8GeV
    sim.biasing_operators = [ bias_operators.PhotoNuclear('old_ecal',550.,
                                        4500.,only_children_of_primary =
                                        True) ]

    # the following filters are in a library that needs to be included
    includeBiasing.library()

    # Configure the sequence in which user actions should be called.
    sim.actions.extend([
            filters.TaggerVetoFilter(),
            # Only consider events where a hard brem occurs
            filters.TargetBremFilter(),
            # Only consider events where a PN reaction happnes in the ECal
            filters.EcalProcessFilter(),
            # Tag all photo-nuclear tracks to persist them to the event.
            util.TrackProcessFilter.photo_nuclear()
    ])

    return sim
```

```
def kaon_pn( detector, generator ) :
    """Adding kaon filtering to the above photo_nuclear generator

    Parameters
    ----------

    detector : str
        Path to the detector
    generator : PrimaryGenerator
        generator to use

    """

    # Instantiate the simulator.
    sim = simulator.simulator("kaon-pn")

    # Set the path to the detector to use.
    #   the second parameter says we want to include scoring planes
    sim.setDetector( detector , True )

    # Set run parameters
    #sim.runNumber = 0
    sim.description = "ECal photo-nuclear,kaon filtering,  xsec bias 550"
    sim.beamSpotSmear = [20., 80., 0.] #mm

    sim.generators.append( generator )

    # Enable and configure the biasing
    #   In order to conform to older samples,
    #   we can only attach to some of the volumes in the ecal
    #   so we ask for this operator to be attached to the 'old_ecal'
    #  biasing factors are 450., 2500. for 4GeV, 550., 4500. for 8GeV
    sim.biasing_operators = [ bias_operators.PhotoNuclear('old_ecal',550.,
                                        4500.,only_children_of_primary =
                                        True) ]

    # the following filters are in a library that needs to be included
    includeBiasing.library()

    # Configure the sequence in which user actions should be called.
    sim.actions.extend([
            filters.TaggerVetoFilter(),
            # Only consider events where a hard brem occurs
            filters.TargetBremFilter(),
            # Only consider events where a PN reaction happnes in the ECal
            filters.EcalProcessFilter(),
            #Filter for events with a kaon daughter
            particle_filter.PhotoNuclearProductsFilter.kaon(),
            # Tag all photo-nuclear tracks to persist them to the event.
            util.TrackProcessFilter.photo_nuclear()
    ])

    return sim
```